Review of the Development of Methods for Characterization of Microspheres for Use in Embolotherapy: Translating Bench to Cathlab

Marcus Caine, Dario Carugo, Xunli Zhang, Martyn Hill, Matthew R. Dreher, and Andrew L. Lewis*

Therapeutic embolotherapy is the deliberate occlusion of a blood vessel within the body, which can be for the prevention of internal bleeding, stemming of flow through an arteriovenous malformation, or occlusion of blood vessels feeding a tumor. This is achieved using a wide selection of embolic devices such as balloons, coils, gels, glues, and particles. Particulate embolization is often favored for blocking smaller vessels, particularly within hypervascularized tumors, as they are available in calibrated sizes and can be delivered distally via microcatheters for precise occlusion with associated locoregional drug delivery. Embolic performance has been traditionally evaluated using animal models, but with increasing interest in the 3R's (replacement, reduction, refinement), manufacturers, regulators, and clinicians have shown interest in the development of more sophisticated in vitro methods for evaluation and prediction of in vivo performance. Herein the current progress in developing bespoke techniques incorporating physical handling, fluid dynamics, occlusive behavior, and sustained drug elution kinetics within vascular systems is reviewed. While it is necessary to continue to validate the safety of such devices in vivo, great strides have been made in the development of bench tests that better predict the behavior of these products aligned with the principles of the 3R's.

1. Microspheres in Advanced Healthcare Applications

Microspheres are small spherical particles with a diameter in the range 1–1000 μm, typically free-flowing in nature that can be made from either synthetic or natural materials (or a combination thereof). They have found widespread use in healthcare applications because numerous methods exist to manufacture them with great control over size, shape, and surface morphology (with potentially large surface areas) and with solid, porous, or capsular internal structures.[1] This provides the ability to encapsulate almost any desired molecule and modulate its release, making the microsphere a common format employed in the design of drug delivery systems.[2] Selection of these various attributes depends upon the intended therapeutic application of the microspheres, which dictates how they are to be delivered, where to, and for how long they should act. For instance, they can be made mucoadhesive in order to promote better contact delivery and long residence times for ocular,[3] nasal,[4] and colonic applications.[5] Magnetic microspheres can be made susceptible to magnetic fields for use in cell isolation, protein purification, and to target drugs to tumors.[6] Low-density systems may be selected for use in oral drug formulations, such as gastro-retentive floating microspheres that enable prolonged drug release in the stomach.[7] Glass microspheres based on Yttrium-90 have been made radioactive for use in localized radiation therapy by injection into the arteries of tumors,[8] whereas titanium phosphate glasses have shown promise in bone tissue regeneration.[9] Polymeric microspheres have been widely used for peptide, protein, hormone, and vaccine delivery, often controlled by biodegradation of the polymer matrix.[10] In some applications however, it is the physical properties of the microspheres themselves that facilitate their mode of action, for instance, in their use as tissue bulking and filling agents, for augmentation of defective sphincters,[11] closure of fistulas,[12] and for intra-arterial delivery to occlude blood vessels. In this latter application it is other, less well-studied properties of the microspheres that become important, such as their physicomechanical properties, buoyancy, and behavior under flow. In this review, we focus on the growing number of novel methods reported in the literature for aiding the characterization and development of novel microspheres for use in embolotherapy.

1.1. Therapeutic Embolotherapy with Microspheres

Over the past 30 years, the practice of interventional radiology has moved from being more diagnostic in nature, to include therapeutic intent using image-guided catheter-directed techniques. Given the benefits of such a treatment paradigm one might

M. Caine, Dr. D. Carugo, Dr. X. Zhang, Prof. M. Hill
Faculty of Engineering and the Environment
University of Southampton
University Road, Highfield, Southampton SO17 1BJ, UK
E-mail: marcus.caine@btgplc.com
M. Caine, Dr. M. R. Dreher, Prof. A. L. Lewis
Biocompatibles UK Ltd., Lakeview
Riverside Way, Watchmoor Park, Camberley GU15 3YL, UK

DOI: 10.1002/adhm.201601291

© 2017 WILEY-VCH Verlag GmbH & Co. KGaA, Weinheim

consider the practice an open and shut case and indeed many of the currently performed procedures focus on minimally invasive treatments that either aim to restore the flow of blood, bile, or urine to an end organ, or on the blockage of blood flow at a target site to bring about a therapeutic effect—known as embolotherapy.[13] As practice has developed, advancements in imaging, catheter technologies, and the myriad of medical devices available to the interventionalist have meant that treatments have become more sophisticated and effective. The devices that have been developed to enable targeted occlusion of blood vessels have likewise undergone a similar evolution in design.

In the early days, physicians would use almost anything that could be squeezed down a catheter in order to cause an obstruction in the vessel, such as autologous blood clot or the use of gelatin sponge pieces passed between two connected syringes to produce a slurry.[14] Polyvinyl alcohol (PVA) foam was the first commercially available synthetic particulate embolization agent,[15] selected because of the wide medical application and known biocompatibility of the material.[16] The particles were sieved into size ranges to provide the interventional radiologist with a choice of agent depending upon the size of the vessels to be occluded.[17] The commercial availability of microspherical embolization agents occurred some years after the appearance of particulate PVA in the mid-1990s with the launch of the Embosphere microspheres (then BioSphere Medical, now Merit Medical[18]). Over the next few decades a range of many different types of microspherical embolization agents reached the market, with ever-increasing functionality such as expanded size range availability, drug loading and elution capability, degradability, and more recently, X-ray imageability (**Table 1**). With so many different material compositions involved, manufacturers have had to design more complex methods of characterization and evaluation to aid in the development and regulatory approval of these devices. An excellent introductory two-part review was conducted by Giunchedi et al. of the various microsphere chemistries and their unique properties, with a comparison to conventional Lipiodol-based transarterial chemoembolization (cTACE).[19] Since this time there have been several noteworthy additions to the field such as biodegradable microspheres,[20] significantly reduced average sizes,[21] and radiopaque microspheres.[22] Here we attempt to pull together for the first time a review of the published literature pertaining to the methods and techniques applied to the translation of embolic agent performance from bench testing to eventual clinical application.

2. Measuring Microsphere Physicochemical/Mechanical Properties and Their Impact on Occlusion Behavior

There are multiple parameters that have significant influence on the performance of the embolic agent (**Figure 1**), which are somewhat interrelated with one another.

2.1. Microparticle Shape

Particulate nonspherical PVA is still used today for many procedures given its relative cost effectiveness and proven clinical history.[15,17] It can, however, be complicated to administer through some of the newer small caliber lumen microcatheters, as the irregular shape of the particles means they tend to interlock and occlude the lumen if not delivered very slowly and in dilute suspension.[23] This tendency for aggregation and more proximal occlusion was not predicted using bench testing but was demonstrated in animal studies, which also showed that microspherical embolization agents did not tend to aggregate given their smooth surface morphology and were carried by blood flow into more distal locations.[24] Optical microscopy

Marcus Caine is a Senior Innovation Scientist at Biocompatibles UK Ltd., part of the BTG group. His role centers on primary interaction with treating physicians for training and research exchange, he is also completing a part-time Ph.D. with the University of Southampton in Applied Biomimetic Microfluidics. This research project focuses on the application of in vitro research methods for advancing treatment efficacy in the fields of interventional oncology and pulmonology.

Dario Carugo is a New Frontiers Fellow in the Faculty of Engineering and the Environment at the University of Southampton. In Southampton he obtained a Ph.D. in Bioengineering Sciences in 2012, and then worked as a postdoctoral researcher at the University of Oxford. His research focuses on the development of microscale systems to investigate or induce therapeutically relevant effects, with potential for clinical or industrial translation.

Andrew L. Lewis is Director of R&D in Innovation at BTG. He specializes in the development of advanced biomedical polymer systems, for instance, to enhance the biocompatibility of implants or to modulate delivery of active agents in the body. These technologies have been applied to novel drug–device combination products for use in interventional therapies in the treatment of cardiovascular disease and cancer.

© 2017 WILEY-VCH Verlag GmbH & Co. KGaA, Weinheim

Table 1. Overview of commercial embolization microspheres currently available in the market (at the time of this review). For each agent, material composition, size, and other specific properties are reported.

Product	Materials composition	Sizes available [μm]	Specific properties
		Nonspherical particulate embolization agents	
Particulate PVA Many available, e.g., Bearing (Merit Medical)	Polyvinyl alcohol foam particles	45–150, 150–250, 250–355, 355–500, 500–710, 710–1000, 1000–1180	Particulate, nonspherical, nonabsorbable
LC Bead (BTG)	Acrylamido-polyvinylalcohol-AMPS hydrogel microspheres	70–150, 100–300, 300–500, 500–700	Spherical, calibrated sizes, nonabsorbable, contain sulfonate binding groups
LC Bead LUMI (BTG)	Triiodobenzyl-modified acrylamido-polyvinylalcohol-AMPS hydrogel microspheres	70–150, 100–300	Spherical, calibrated sizes, nonabsorbable, X-ray visible, contain sulfonate binding groups
Gelfoam (Pfizer)	Purified pork skin gelatin sponge	Milled powder or sheets	Powder used for hemostasis, sheet may be cut into small pledgets or made into a slurry and used off-label as resorbable temporary embolic
		Microspherical embolization agents	
Degradable starch microspheres (DSM), e.g., Embocept (Pharmacept)	Amilomer (hydrolyzed potato starch)	≈50	35 min half-life, degraded by blood amylases
Gel-Bead (Vascular Solutions)	Gelatin microspheres	100–300, 300–500, 500–700, 700–1000	Degradation in 4–12 weeks
Occlusin 500 (ImbioTechnologies)	Collagen-coated poly(lactic-*co*-glycolic acid) microspheres	212	Degradable in 12–24 weeks
Embosphere (Merit Medical)	Tris-acryl gelatin microspheres	40–120, 100–300, 300–500, 500–700, 700–900, 900–1200	Spherical, calibrated sizes, nonabsorbable
Bead Block (BTG)	Acrylamido-polyvinylalcohol hydrogel microspheres	100–300, 300–500, 500–700, 700–900, 900–1200	Spherical, calibrated sizes, nonabsorbable, tinted blue
Embozene (Boston Scientific)	Poly(methylacrylic acid) microspheres coated with Polyzene-F	40, 75, 100, 250, 400, 500, 700, 900, 1100, 1300	Spherical, calibrated sizes, nonabsorbable, tinted different colors, with biodegradable coating
HydroPearl (Terumo)	Polyethylene glycol-based microspheres	75, 200, 400, 600, 800, 1100	Spherical, calibrated sizes, nonabsorbable, tinted different colors
X-Spheres (Interface Biomaterials)	Triiodobenzyl-modified acrylic microspheres	400–600, 600–710, 710–850	Spherical, calibrated sizes, nonabsorbable, tinted yellow, X-ray visible
		Drug eluting microspherical embolic agents	
DC Bead (BTG)	Acrylamido-polyvinylalcohol-AMPS hydrogel microspheres	70–150, 100–300, 300–500, 500–700	Spherical, calibrated sizes, nonabsorbable, CE marked for loading with doxorubicin and irinotecan, Contain sulfonate binding groups
HepaSphere/QuadraSphere (Merit Medical)	Poly(vinyl alcohol-*co*-acrylic acid) microspheres	30–60, 50–100, 100–150, 150–200	Calibrated, dry microspheres which swell 4× in saline, CE marked for loading with doxorubicin and irinotecan, contain carboxylate binding groups
Tandem/Oncozene (Boston Scientific)	Poly(methylacrylic acid) microspheres coated with Polyzene-F	40, 75, 100	Spherical, calibrated sizes, nonabsorbable, white, capable of drug loading, contain carboxylate binding groups.
LifePearl (Terumo)	Polyethylene glycol-AMPS based microspheres	100, 200, 400	Spherical, calibrated sizes, nonabsorbable, tinted green, capable of drug loading, contain sulfonate binding groups
DC Bead LUMI (BTG)	Triiodobenzyl-modified acrylamido-polyvinylalcohol-AMPS hydrogel microspheres	70–150, 100–300	Spherical, calibrated sizes, nonabsorbable, contain sulfonate binding groups

is one of the few methods that has been used to characterize particulate PVA and has shown that it can often be associated with smaller than calibrated sizes that could potentially cause off target distal embolization.[7] Nevertheless, PVA still finds widespread use where simple proximal mechanical occlusion is desired, such as for treating arterial hemorrhage[25] and arteriovenous malformations.[26] Where the physician has a desire for the embolic agent to be more flow-directed to achieve deeper penetration and a more predictable occlusion location, microspherical embolization agents will tend to be used. Moreover,

© 2017 WILEY-VCH Verlag GmbH & Co. KGaA, Weinheim

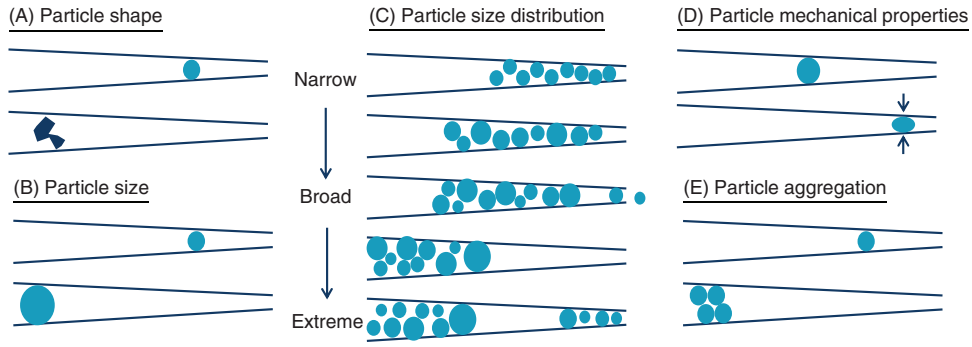

Figure 1. Highlighting confinement effects, A) shape, B) size, C) frequency distribution, D) mechanical properties, and E) the presence of aggregation as primary parameters influencing microsphere occlusion.

microspheres loaded with chemotherapeutic agents, or so called drug-eluting beads (DEBs) are usually used for more distal penetration of malignant tumors, for instance, in order to deliver a local sustained dose of drug within the tumor feeding vessels.[27]

2.2. Microsphere Composition

Table 1 outlines the commercial embolization microspheres currently available at the time of this review. Naturally, not all of the microspheres outlined are manufactured using the same methodology, and each process utilizes different basic chemical constituents. The formulation composition for a microsphere influences the physicochemical properties that it exhibits and this can be tailored to produce specifically desired attributes such as compressibility, radiopacity, drug binding capacity, and biodegradability. It will also, however, influence the surface properties and hence tendency to interact and aggregate, and bulk properties such as density and water content which will affect how the microspheres suspend in solution, their rate of sedimentation, their ability to pass through narrow microcatheter lumens, and their subsequent behavior in blood flow and at the eventual site of occlusion. In the following sections we will outline how some of the key microsphere attributes are measured and then focus on each of the steps performed in the preparation and administration of microspherical embolization agents and how differences in physicochemical properties between products influence their behavior.

2.3. Microsphere Size and Size Distribution

Obviously the size of the microsphere is somewhat critical in the determination of the size of the vessels that are embolized, not only as it is a major determinant of the fluid dynamic behavior of the microsphere (Table 5) but also because it dictates the level of occlusion in the vasculature (Figure 1B). Few of the commercially available embolic microspheres are one size only, most being supplied as either a narrow or broad size distribution within a range (since the vessels in a targeted location are also a distribution of sizes). Comparison of narrow versus broader size distribution microspheres of the same chemical composition (nominal sizes of both 600 and 800 μm) in kidney and uterus animal models showed there to be no difference in the distribution of the broad versus narrow size ranges in vivo, and hence no targeting advantage for narrower size ranges.[28] Smaller microspheres (<100–300 μm) however, do distribute differently in vivo, the smaller size range penetrating deeper into the vasculature, as there is less chance of a larger microsphere blocking the vessel first and impeding the passage of subsequent microspheres.[29]

Size is most commonly measured using optical microscopy, sometimes with calibrated software that allows accurate measurement of microsphere diameter in a particular field of view, with usually a minimum number of 200 measurements to produce a representative histogram of the distribution of size within the range.[21] As most of the microsphere products on the market are sieved into size fractions, the resulting histograms for each size fraction are not necessarily normally distributed, and can often be skewed to the lower or upper end of the distribution, although the minimum and maximum sizes in the range are the same. For example, **Figure 2** shows a histogram for the size distribution of DC Bead (1000 measurements over five lots) showing how the 70–150 μm size range is a subset of the 100–300 μm size range with the same minimum microsphere size.[21] Interestingly, it has been shown that some

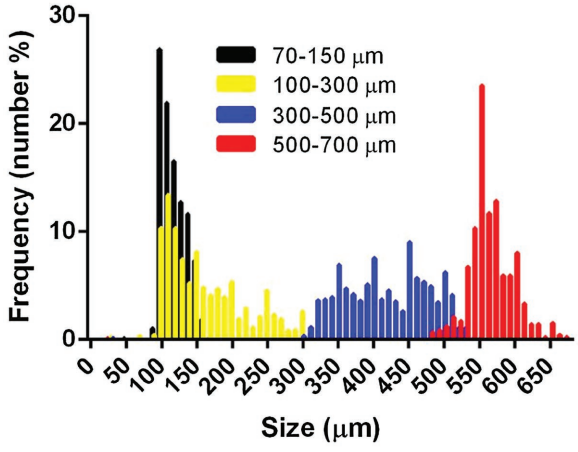

Figure 2. Histogram of the size distributions (by frequency) for the four commercially available size ranges for DC Bead. Beads were sized from microscope images. Reproduced with permission.[21] Copyright 2016, Springer.

© 2017 WILEY-VCH Verlag GmbH & Co. KGaA, Weinheim

of the reported size distributions for the products with supposed tighter calibration are not as they are claimed with significant numbers of microspheres outside of the manufacturer's labeled size specification.[30] Scanning electron microscopy (SEM) has also been used to characterize microspheres for surface morphology and size[31] but care must be taken with the introduction of visual artifacts caused in the high vacuum environment of the SEM that would dehydrate hydrogel microspheres rapidly, for instance, without some fixation process.[31a]

A simple wedge-geometry glass plate model has been reported that allows simple visualization of microsphere penetration potential, which can clearly demonstrate localization of different size ranges (Figure 8).[21] The absolute level of occlusion is not representative of what is observed in vivo as microsphere compressibility is also an important property that influences how distal a microsphere may travel (Figure 1D). In the plate model, the microsphere is allowed to compress uniaxially instead of radially as it would when confined in a vessel; but the relative levels of penetration remain predictive of the in vivo performance. In poorly designed and characterized products, changes in the compressibility of the microsphere between different size ranges can lead to mechanical properties that dominate over size in determining size of occluded vessels, resulting in unpredictable performance.[30] Where the microsphere is a DEB the model also allows the comparison of performance between bland and drug-loaded microspheres.[21] With some DEBs the loading of the drug results in a decrease in the average diameter of the microsphere by as much as 30% (depending upon dose loaded)[32]; but this is also accompanied by a concomitant increase in the elastic modulus of the DEB which offsets the size change and means the penetration potential remains largely the same.[21,33]

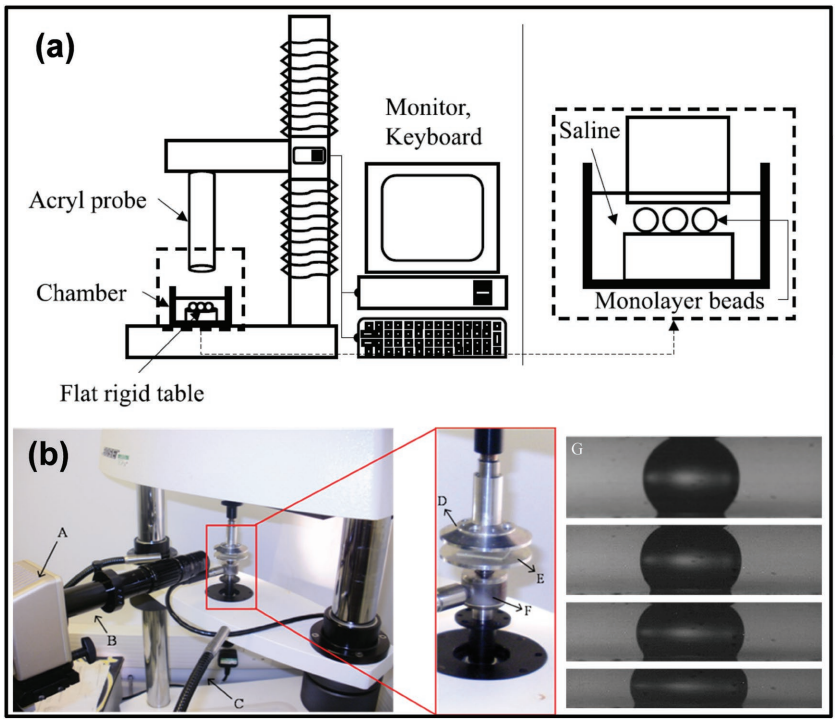

Figure 3. a) Experimental setup for multiple microsphere compression and relaxation testing using a texture analyzer with expanded view of the compression chamber on the right[35b]; b) Photograph of a Bose compression tester for single-microsphere compression: A) high speed camera, B) optical lenses, C) fiber optic, D) compression top plate, E) compression bottom plate, F) force sensor, and G) photographs of a single microsphere during four stages of compression. Reproduced with permission.[78b] Copyright 2012, University of Southampton.

2.4. Microsphere Mechanical Properties

As mechanical properties are clearly a very important determinant of the occlusive behavior of microspherical embolics, many different micromechanical test methods have been described in order to differentiate and predict product performance, in which either single beads[22a,34] or more commonly a monolayer of beads,[32a,33,35] are compressed by a probe (**Figure 3**). Single-microsphere compression is possible using nanoindentation methods but this procedure is challenging for very small microspheres.[22a] Measurement of the Young's modulus of a monolayer of microspheres is possible to give an estimate of microsphere stiffness, but limitations of the methodology means that this works best for larger microspheres or where the size distribution is very narrow.[33] Overall, method-to-method variability is very high and dependent upon many operating factors, so testing needs to be conducted with known benchmarks to provide any meaningful comparative data (**Table 2**).

Microsphere elasticity is also important, as the ability for the microsphere to recover its original size (i.e., after injection using microcatheters) is critical for predictable behavior.[35b] Contour SE was a microspherical embolic agent that failed to work clinically in the treatment of uterine fibroids.[36] Its internal structure was shown to be highly macroporous and sponge-like, as opposed to the microporous nature of hydrogel-based microspheres.[31a] Mechanical studies showed it to be very soft and deformable[31a] but more crucially, once compressed within the microcatheter lumen it did not recover its original size and shape quickly, and caused more distal penetration than expected.[31a]

Hydrogel-like microsphere products demonstrate good levels of compressibility for ease of delivery but are also very elastic, recovering their target dimensions once they have exited the microcatheter.[35b] The ability to deform however, is a feature that must be considered during use of the product, as it is known that many microspherical embolization agents demonstrate a vascular redistribution phenomenon.[37] This may occur when an endpoint has been reached during the embolization where apparently no more product can be administered into the vessels without fear of reflux (retrograde flow and potential off-target embolization).[38] It has been observed however, that if one waits for 5–15 min and then performs another diagnostic

© 2017 WILEY-VCH Verlag GmbH & Co. KGaA, Weinheim

Table 2. Selection of embolic microspheres, their size range (prior to drug loading), drug dose loaded (if applicable), and elastic modulus.

Product[a)]	MS size	Test method	Elastic modulus [kPa]	Reference
LC Bead	100–300 μm	Single bead	110 ± 20	Duran[22a]
LC Bead LUMI	100–300 μm	Single bead	27 200 ± 5460	Duran[22a]
EmboSphere	900–1200 μm	Monolayer	39.6 ± 5.05	Hidaka[35b]
Bead Block	900–1200 μm	Monolayer	18.8 ± 4.00	Hidaka[35b]
Embozene	900 μm	Monolayer	13.6 ± 1.98	Hidaka[35b]
EmboSphere	700–900 μm	Single bead	19.33 ± 4.97	Hidaka[34]
HepaSphere	300–350 μm (dry)	Single bead	9.64 ± 2.46	Hidaka[34]
EmboSphere	900–1200 μm	Monolayer	14.8 ± 0.8	Forster[35d]
Bead Block	900–1200 μm	Monolayer	11.1 ± 0.8	Forster[35d]
DC Bead	900–1200 μm	Monolayer	17.1 ± 1.2	Forster[35d]
Contour SE	900–1200 μm	Monolayer	3.5 ± 1.4	Forster[35d]
DC Bead + Dox (25 mg)	500–700 μm	Monolayer	15.3 ± 3.4	Jordan[32a]
DC Bead + Iri (50 mg)	500–700 μm	Monolayer	7.3 ± 1.2	Jordan[32a]
HepaSphere + Dox (25 mg)	100–150 μm (dry)	Monolayer	11.5 ± 0.9	Jordan[32a]
HepaSphere + Iri (50 mg)	100–150 μm (dry)	Monolayer	2.9 ± 0.7	Jordan[32a]
DC Bead	500–700 μm	Monolayer	5.5 ± 0.02	Jordan[32a]
HepaSphere	100–150 μm (dry)	Monolayer	1.6 ± 0.3	Jordan[32a]
DC Bead + Iri (50 mg)	900–1200 μm	Monolayer	38.0 ± 5.0	Taylor[35c]
DC Bead + Iri (50 mg)	700–900 μm	Monolayer	48.0 ± 10.5	Taylor[35c]
DC Bead + Dox (45 mg)	700–900 μm	Monolayer	248.9 ± 43.9	Lewis[33]
DC Bead + Dox (37.5 mg)	700–900 μm	Monolayer	168.0 ± 18.7	Lewis[33]
DC Bead + Dox (20 mg)	700–900 μm	Monolayer	66.1 ± 6.3	Lewis[33]
DC Bead	700–900 μm	Monolayer	33.0 ± 2.9	Lewis[33]
EmboSphere	700–900 μm	Monolayer	27.6 ± 3.8	Lewis[31a]
Bead Block	700–900 μm	Monolayer	24.1 ± 1.62	Lewis[31a]
Contour SE	700–900 μm	Monolayer	4.48 ± 1.88	Lewis[31a]
EmboGold	700–900 μm	Monolayer	21.0 ± 2.48	Lewis[31a]

[a)]Value in brackets is dose of drug mL^{-1} of microspheres.

angiogram, the vessels appear to have opened again and more embolic agent can be administered.[22b] This effect may be due to temporary crowding of microspheres at a bifurcation followed by the migration of the microspheres to a more distal location under the back pressure of the blood on the occlusive mass, together with some compression of the hydrogel microspheres themselves leading to a more deformed geometry within the vessel.[39]

For DEBs it has been shown from compression tests that the Young's modulus increases with increasing dose of drug loaded into the microsphere (the extent of which depends on the type of microsphere, the drug species, and the dose of drug loaded).[32a,b,33,35e] This increase in stiffness can be quite marked where the drug has the ability to interact with itself, such as is the case with the anthracycline chemotherapeutics, which can π–π stack when in close proximity with each other within the microsphere structure,[40] effectively cross-linking the hydrogel matrix.[33] Indeed, drug loading also reduces water content within the hydrogel which can also affect the density and hence suspension of the product.[22a,33] The presence of drug may also alter the surface characteristics and affect the tendency of the microspheres to aggregate under flow or within the delivery syringes.

2.5. Microsphere Aggregation

PVA particles aggregate more proximally due to their irregular shapes that interlock and form clumps. Microspheres are designed to have smooth surfaces that resist interaction with one another under flow until they are trapped together in a vessel by virtue of size. Aggregation is therefore usually to be avoided as it may complicate delivery and make predictability of occlusion difficult (Figure 1E). One product however, actively utilizes aggregation in its mode of action. Occlusin 500 has a collagen coating which actively binds platelets when introduced into the bloodstream, promoting aggregation of the microspheres which may stabilize the resulting platelet-rich clot that forms.[20c] This product is 212 μm in size and noncompressible, but behaves in vivo in a similar fashion to a 300–500 μm

© 2017 WILEY-VCH Verlag GmbH & Co. KGaA, Weinheim

Tris-acryl gelatin microsphere (TGMS), due to the platelet-induced aggregation.

2.6. Microsphere Degradation

While many of the embolic microspheres used in the clinic are permanent implants, a number of degradable materials are also available. Gelfoam slurry or pledgets have been used for many years as a temporary embolization agent but embolize proximally due to their largely heterogeneous and irregular shape. Gelatin-based microspheres have been proposed for many years as a calibrated solution for embolization[41] and most recently Gel-Beads (Vascular Solutions Inc.) have appeared on the U.S. market which claim to absorb on the body over time, although no data are available yet on the performance of this product. Degradable starch microspheres (DSM) have been available since the early 1980s and initial in vitro evaluation in blood showed them to degrade in 20–30 min due to the presence of serum amylase.[42] Calcium alginate microspheres have been described in which degradation was followed in vitro by measuring calcium loss, size change, and weight loss over time.[35d] Microspheres composed of oxidized carboxymethyl cellulose and carboxymethyl chitosan have been described in which in vitro degradation has been modeled by measurement of weight loss and optical microscopy following incubation in lysozyme to mimic enzymatic action in the body.[20a,b,43] Others have reported on poly(ethylene glycol) methacrylate hydrolysable microspheres for transient vascular embolization in which they monitor weight loss during incubation but also collect the hydrolytic degradation products and analyze them with ^{1}H nuclear magnetic resonance spectroscopy for chemical identification, and extracts are subjected to cell-based contact toxicity assays to test for potential cytotoxicity.[44] Ultimately, for all of these degradable materials, mid-to-long-term implantations in vivo are required to determine actual rate of degradation and local toxicity effects.[20b,c,45]

2.7. Microsphere Radiopacity

Embolic microspheres with intrinsic radiopacity have been described for many years with a multitude of experimental studies in the literature. Radiodensity has been introduced into the microspheres by incorporation of metals such as tantalum, barium, and iron, or addition of organic compounds containing iodine species.[46] While this results in the material being able to absorb X-rays, it can also adversely affect handling and administration of the microspheres due to rapid sedimentation resulting from the increased density.[47] Some of these issues have now been overcome with recent entrants into the market such as X-Spheres, LC Bead LUMI, and DC Bead LUMI. A simple estimate of radiopacity can be gained by subjecting the microspheres to a standard X-ray together with an aluminum step-block to provide a gauge to the degree of visibility. More sophisticated techniques include the preparation of phantoms of the microspheres (**Figure 4**), in which they are suspended in a temperature-sensitive gel such as agar at various concentrations to determine the extent of visibility of different dilutions of microspheres under either high-resolution microcomputed tomography (micro-CT) or under clinically relevant conditions using multidetector CT (MDCT).[29,48] Phantoms can also be constructed by packing microspheres into small tubes of varying diameters (line phantoms) to emulate the filling of vessels in order to evaluate the smallest vessels that may be visualized when embolized with the radiopaque microspheres.[22a] Where the microsphere contains iodine as the radiopaque element, total iodine content can be obtained from standard combustion elemental analysis. Moreover, it has also been demonstrated that iodine distribution can be measured by embedding and sectioning the microsphere using a microtome, followed by imaging with a SEM to select a survey line across the diameter of the sectioned sphere, followed by use of energy dispersive X-ray analysis (EDAX) to determine elemental composition across the survey.

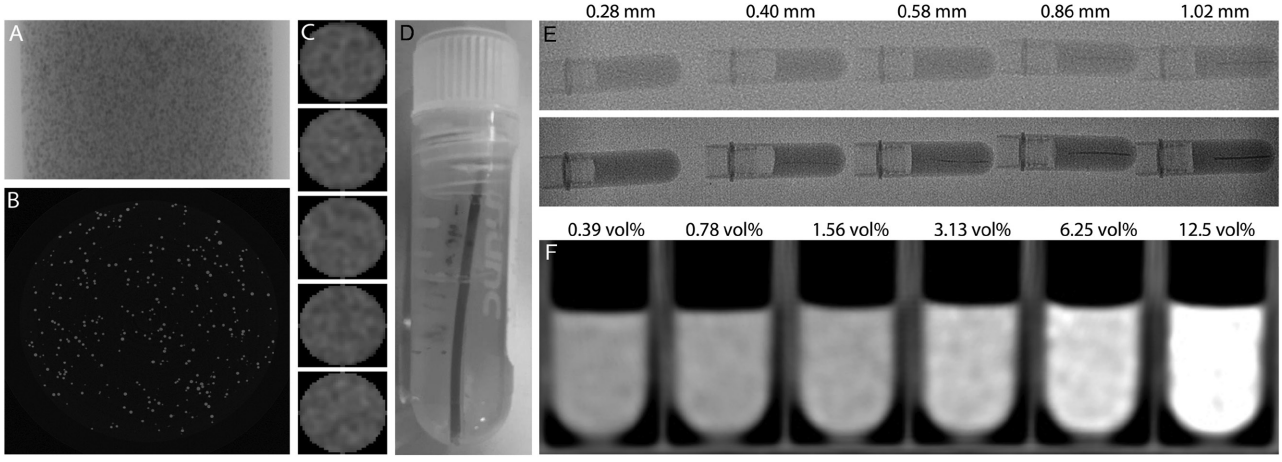

Figure 4. A) X-ray image through a section of a phantom showing radiopaque microspheres suspended in gel; B) micro-CT cross section through the gel showing uniform radiopacity for the microspheres; C) typical micro-CT reconstructions for five representative microspheres; D) photograph of a line phantom of radiopaque microspheres; E) line phantoms of different line diameters under fluoroscopy (top line) and single shot (higher energy, lower line) X-ray; F) MDCT images of different concentrations of microsphere suspensions from 0.39 to 12.5 vol%, showing the relationship between radiopacity and suspension dilution. Reproduced with permission.[22a] Copyright 2006, the authors, published under CC-BY-NC license.

© 2017 WILEY-VCH Verlag GmbH & Co. KGaA, Weinheim

With some basic characterization techniques described in this section, the following sections take a more detailed look at the steps involved in the preparation of embolic agents and their subsequent delivery into the body, including aspects of drug loading and elution for DEBs where relevant.

3. Suspension, Handling, and Microcatheter Delivery of Microspheres

When discussing the application of testing methods to embolic devices it becomes important to consider the intended mode of action.[38b,49] The process of delivering embolic devices has many discrete considerations, including preparation, ensuring adequate physical suspension of the embolic material during delivery via appropriately positioned microcatheters, to characterizing the resistance observed during delivery (**Figure 5**). Required product attributes include minimal fragmentation, ease of delivery (low resistance), and conformance to the microcatheter during delivery.[49a]

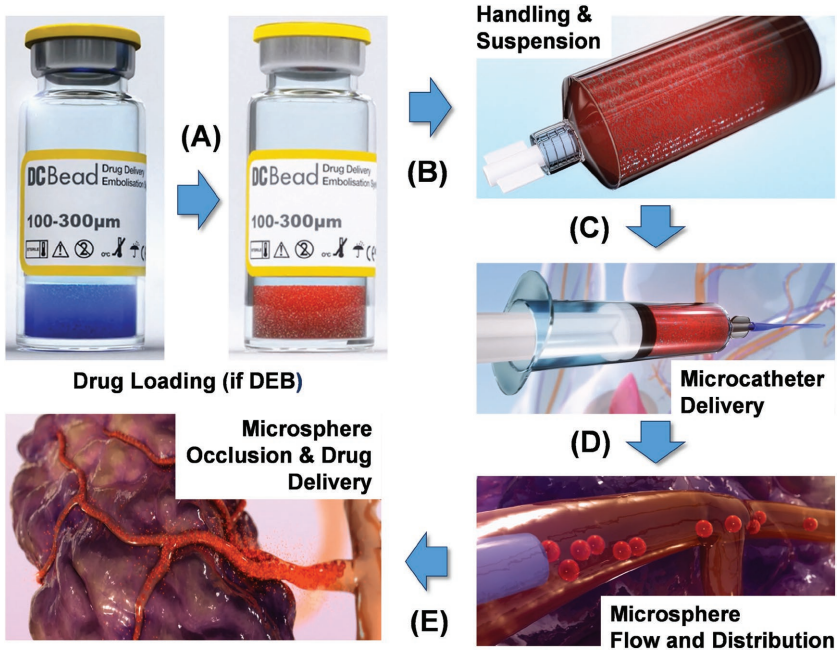

Figure 5. Different stages in the preparation of drug-loaded microspheres. A) Ionic drug loading, B) handling and even suspension in contrast agent, C) administration via microcatheter, D) allowing free-flowing microsphere distribution in the blood stream leading to E) vessel occlusion and local drug delivery.

3.1. Ensuring Optimum Suspension

Depending on surface chemistry and morphology of microspheres, their physical introduction via microcatheter will require adequate suspension to minimize occlusion within the confined hub of the catheter. This is typically achieved using a viscous radiopaque contrast agent which reduces the occurrence of embolic aggregation. There are a wide range of contrast agents available for use with various densities, viscosities, and additive chemistries, however there is currently no clearly defined scientific rationale for selection of type.

The suspension characteristics of microspheres are typically assessed using time to loss of suspension within a syringe. This is impacted by the relative density, osmolality, and viscosity of the microsphere suspension and their suspending medium, and is of great practical importance as it defines the injection period before resuspension is required by the physician.[50] Different microspheres will therefore have unique suspension properties and will interact differently in certain contrast media types. **Table 3** is an example of Bead Block suspension in four major contrast agents highlighting the variations of suspension time relative to dilution ratio.

Although not fully comprehensive, characterization of bench top performance can be used to identify trends in physicochemical performance for a given product. The physical properties of a microsphere suspension will also impact the handling during delivery and potentially the distribution of microsphere suspensions in vivo. The ability of the physician to consistently administer the suspension will also be a significant factor in evaluating the performance of the composition. The chemical properties of contrast agents can also influence the chemical stability and elution properties of drug-loaded microspheres and any ionic interaction must be carefully analyzed prior to use.[51] For example, contrast agents with high ionic contents such as Visipaque (GE Healthcare) have been shown to be associated with rapid elution of some ionically bound drugs.[52] Chemical stability and chromatographic purity are determined from high-performance liquid chromatography (HPLC) testing

Table 3. Time required to create a durable suspension of Bead Block microspheres in contrast agent by size and contrast agent type with dilution volume shown below.

Bead Block Size range [µm]	Indication	Omnipaque 300	Isovue 300	Optiray 300	Visipaque 320
100–300	PAE hypervascular tumors	1 min (in 5 mL)	1 min (in 5 mL)	1 min (in 5 mL)	1 min (in 5 mL)
300–500	PAE hypervascular tumors	2 min (in 5 mL)	1 min (in 5 mL)	1 min (in 5 mL)	2 min (in 5 mL)
500–700	UFE hypervascular tumors	3 min (in 5 mL)	2 min (in 5 mL)	2 min (in 5 mL)	5 min (in 4 mL)
700–900	UFE hypervascular tumors	5 min (in 5 mL)	4 min (in 5 mL)	4 min (in 5 mL)	5 min (in 2 mL)
900–1200	UFE hypervascular tumors	3 min (in 2 mL)	3 min (in 2 mL)	4 min (in 2 mL)	6 min (in 2 mL)

© 2017 WILEY-VCH Verlag GmbH & Co. KGaA, Weinheim

of drug compounds, this can then be used to issue recommendations regarding the storage and use of drug-loaded microsphere suspensions.[51]

Blood interaction in terms of relative viscosity and erythrocyte aggregation was also studied with various contrast agent types.[50,53] It was shown that with increasing contrast agent viscosity could lead to inhomogeneous distribution of suspended particles due to shear-induced erythrocyte aggregation.[50] The physicochemical properties of the chosen contrast agent will also need to be tailored to the physical properties of microspheres. The recently developed radiopaque microspheres, which are chemically modified to yield inherent radiopacity, also present increased density and lower compressibility as a result of the chemical iodination process.[22a] It is therefore increasingly important to match suspension properties of the contrast agents to those of the microspheres, in the case of microspheres with higher density, by increasing the viscosity and density to reduce the sedimentation effect over time.[22a] Profiling and evaluation of these chemical changes is not always possible with conventional in vitro methods. Therefore, applied flow models that incorporate measures of suspension, administration, and flow distribution increase understanding of any potential effects, for example, in evaluating a novel microsphere prior to preclinical evaluation.

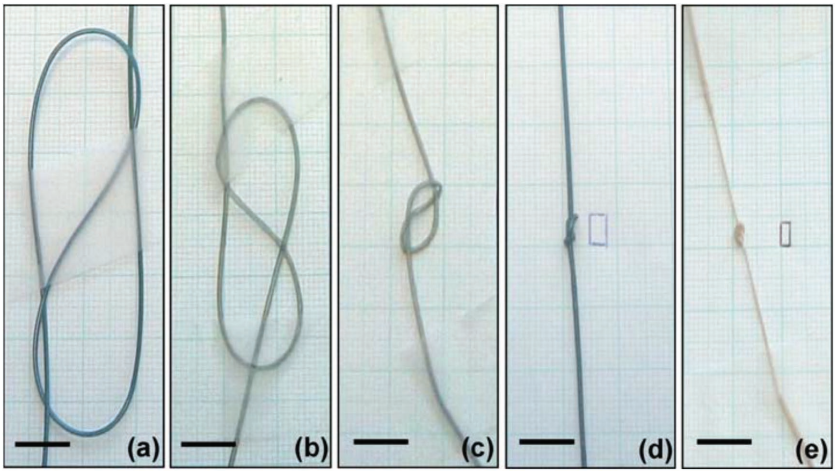

Figure 6. Tortuosity loops used to assess catheter deliverability: a) 6.5 × 2, b) 4.5 × 1.5, c) 1.5 × 0.8, d) 0.5 × 0.3, and e) 0.4 × 0.2 cm (scale bar = 1 cm). Reproduced with permission.[31a] Copyright 2006, Springer.

3.2. Handling and Microcatheter Delivery

Historically, catheter compatibility was assessed using multiple operators and various catheter types and sizes in tortuous and straight configurations. The deliverability of embolics was then assessed using ranked operator feedback.[32b,54] As embolotherapy has developed so too have microcatheter designs and functionality. The physical size and internal diameter of catheters has been significantly reduced over the past 20 years to enable increased superselective targeting of small vessels with controlled positioning, while surface modification of the inner lumen and antikinking technology have reduced risk associated with thrombogenicity and terminal blockages.[55]

The physicochemical properties of microsphere suspensions have also been associated with the miscibility and distribution within hemodynamic flow.[56] It has been proposed that microspheres will track to the distribution of injected solutions in blood.[57] Although recent investigation into the discrete distribution profiles of different radioembolic microspheres has indicated that there may be an inconsistency with the hemodynamic blood distribution pattern predicted in these studies,[58] instead particles may distribute as a discrete phase that has the potential for tailored alignment through incorporation of contrast agent.[76] This theory was previously only supported through ex vivo histology for microsphere location following administration, now it is possible through the use of radiopaque microspheres to characterize the real-time flow distribution as this aligns with contrast agent distribution.[76] This offers the ability to align distribution effects with suspension durability for in vitro–in vivo correlations.

In creating additional metrics for evaluation of the delivery conditions it is important to understand the potential implications in a clinical scenario. This has been demonstrated with the Surefire Infusion System (Surefire Medical Inc., USA) and its proposed ability to increase the accuracy of distal embolic delivery and minimization of embolic reflux.[59] The claim of the device is the prevention of retrograde flow or reflux following distal embolization, through the use of an inflatable hood at the tip of the catheter. Initial validation and assessment of this delivery device was performed in terms of the blood pressure as a precursor to activation of the device.[59,60] The antireflux catheter system has also been employed in delivery of radioembolization.[59b,60] This therapy is highly flow dependent as there is a minimal level of embolic effect, the hemodynamics within the selected vascular path must thus ensure effective distribution of suspended microspheres.

Tortuous path microcatheters have been utilized for evaluating the morphological attributes of different microspheres and their effect on deliverability. This involves the forced kinking of the microcatheter to impose a confinement effect (**Figure 6**) and test the deformation and elasticity of microspheres during delivery.[31a] The physical compatibility of microspheres has been profiled and has started to be publicly reported to provide confidence in specific product combinations and to highlight limitations prior to procedural use. Notably, it is important to design handling studies with the end user in mind. This has recently been demonstrated during development of novel radiopaque microspheres (**Table 4**) where the investigators conducted a series of handling studies involving both technical and clinical users to ensure that variations in the administration styles and levels of experience were considered when impartially evaluating potential microsphere chemistries.[22a,48a,61] The results of these studies helped in the selection of a candidate that could be used in clinical practice and which was taken forward for further in vivo studies.[22b] Such use of in vitro blinded

© 2017 WILEY-VCH Verlag GmbH & Co. KGaA, Weinheim

Table 4. Catheter deliverability of various sizes of RO beads. With permission from ref. [22a].

RO bead size [μm]	1.9 Fr (ID = 419 μm)	2.3 Fr (ID = 33 μm)	2.4 Fr (ID = 59 μm)	2.8 Fr (ID = 86 μm)	4 Fr (ID = 1003 μm)
40–90	Pass[a)]	Pass	Pass	Pass	Pass
70–150	Pass[a)]	Pass	Pass	Pass	Pass
100–300	Fail	Pass	Pass	Pass	Pass
300–500	Fail	Fail	Fail	Fail	Pass

[a)]40–90 and 70–150 μm delivered using a 1 mL syringe with a 1.9 Fr catheter only. 3 mL syringe was used for larger catheters. ID: inner diameter.

assessment additionally encourages a fit-for-purpose rationale that can then be linked to product training and experience to enhance safety and application.

A recent report by Lu et al. incorporates catheter hub pressure recordings into deliverability studies of novel Lipiodol-containing polyvinyl alcohol microcapsules (LPMs) (**Figure 7**).[62] Static pressure or physical embolic resistance can be a critical measure of the performance of a product suspension. It is proposed that proximal and distal pressure can be utilized to measure the real-time response of microsphere suspensions in terms of embolic characteristics and performance. Recent studies measuring pressure-induced reperfusion[63] and associated intratumoral hypoxia[64] have suggested that pressure at the catheter tip measured through direct in vitro recording could be directly correlated to that of the tumor microvasculature.

Expansion and optimization of an in vitro bench top indicator of the physical ability to restrict fluid flow in confined channels relative to the microsphere chemistry and suspension durability would serve as an evaluative measure of the functional mode of action of different microsphere chemistries and compositions. Through standardization of the testing method it is possible to remove bias associated with operator delivery and increase the confidence in comparative assessment.[38b] Optimization of this process would aid in the effective translation of bench studies to clinical profiling methodologies.

3.3. Microsphere Delivery Considerations

Embolic therapy is regarded as a highly dynamic process where practitioners must tailor the physical handling of the product to the unique vascularity of the patient. This degree of customization has resulted in a lack of consensus regarding the administration style and potential effects.[38b] There have been several studies into the effect of administration rates, suspension, dilution, and catheter positioning as well as the clinical response of these variations stratified by patient type.[49b,65] Results indicated that the volume of product, size, and injection rate can all influence the degree of tumor necrosis and clinical response, for example, Choe et al. found that reducing the delivery rate was associated with higher microsphere delivery volumes prior to stasis within the target vasculature.[65a] This has implications for drug delivery especially, where a calculated dose is required for tumor response.[49b,65] The ability to administer specific microsphere volumes intended to deliver either a precalculated dose of chemotherapeutic drug or to elicit a calibrated physical restriction is heavily determined by physicochemical characteristics of the microspheres.[74b] In cases of proximal occlusion or reflux, underdosing or off-target embolization can result in reduced procedural efficacy or increased risk to the patient.[74b] Slower injection rates have been associated with higher tumor filling and also reduced risk of reflux[57c] whereas positioning of the microcatheter (distal vs proximal) and selection of smaller sizes of embolics has been shown to result in more distal penetration and homogenous tumoral coverage.[29,66]

These effects have been recreated with in vitro testing protocols to confirm specific flow properties in terms of their defining physical properties which have the potential to be used as indicators of performance in vivo. Models to profile the flow and embolic effects resulting from variations in the administration style and embolic material have been developed to specifically define the distribution and embolic profiles of embolic microspheres during administration.

4. Flow Behavior and Occlusion Performance of Embolic Devices

Understanding the flow behavior of embolic devices after injection into the bloodstream is of crucial importance to predict and potentially control the localization of embolic events in

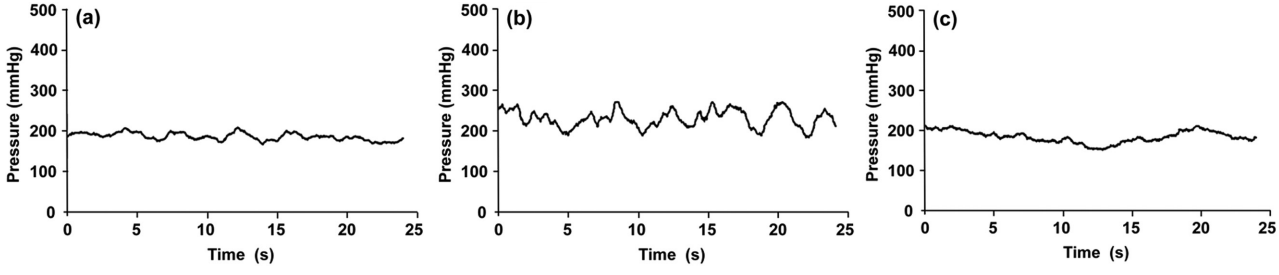

Figure 7. Pressure curves of catheter delivery test for Lipiodol Polymeric Microspheres (LPMs). a) 300–500 μm, 3 Fr; b) 500–700 μm, 3 Fr; and c) 700–900 μm, 4 Fr. Reproduced with permission.[62] Copyright 2013, Elsevier.

© 2017 WILEY-VCH Verlag GmbH & Co. KGaA, Weinheim

Table 5. Relevant forces acting on an embolic particle steadily flowing through a blood vessel. For each type of force, a brief description of its physical meaning, the direction of action relative to the mean flow, and the main physical determinants are reported. These are divided into subcategories depending on whether they are related to the physical properties of blood, blood vessel, or embolic particle. ρ_b = blood density, μ_b = blood dynamic viscosity, v_b = blood velocity, D_h = vessel hydraulic diameter, R_c = vessel radius of curvature, r = radial position of particle within the vessel, v_p = particle velocity, R_p = particle radius, β_p = particle compressibility, ∥ = parallel to, and ⊥ = perpendicular to.

Force type	Physical meaning	Physical determinants			
		Direction of action	Blood	Vessel	Particle
Buoyancy	Force exerted by a fluid that opposes the weight of an immersed object	⊥ mean flow	ρ_b	–	R_p
Weight	Force on a sphere due to gravity	⊥ mean flow	–	–	ρ_p, R_p
Stokes drag	Frictional force exerted on a sphere within a viscous fluid	∥ mean flow	μ_b	–	R_p, $v_p(r)$
Dean drag	Drag force induced by secondary flows associated with curved channels	⊥ mean flow	ρ_b, μ_b, $v_b(r)$	D_h, R_c	R_p
Wall interaction Lift	Force resulting from the hydrodynamic interaction between particle and walls, upon confinement	⊥ mean flow	ρ_b, μ_b, $v_b(r)$	D_h, R_c	R_p, r, β_p
Shear gradient Lift	Force due to the curvature of the velocity profile (i.e., velocity gradient)	⊥ mean flow	ρ_b, μ_b, $v_b(r)$	D_h, R_c	R_p, $v_p(r)$, r, β_p

the tumor vasculature. This is recognized as a primary determinant of therapeutic efficacy,[67] and has attracted increasing interest from researchers and enterprises working in the field of embolotherapy. Embolics traditionally are not visible under X-ray imaging, and only the stream of injected contrast phase is used to identify the location of embolic material during delivery.[29] The ability to visualize flow characteristics in controlled settings has been previously investigated,[29] but no clear system design has been identified for this purpose yet. To this end, studies have generated computational and experimental investigational platforms based mainly on sections of the target anatomy of tumors and tumor bearing organs.

4.1. Evaluating Embolic Flow Behavior

From a fluid mechanic perspective, comprehensive characterization and modeling of embolic particle flow behavior is nontrivial and this is due to various physical factors, including (i) the intricacy and patient-specificity of the tumor vascular network,[68] (ii) the non-Newtonian and biphasic nature of the carrier fluid (i.e., blood or a mixture of blood and contrast agent),[69] (iii) the continuous variation of the local rheological properties of blood along the microvascular bed,[70] and (iv) large differences in the physical properties of embolic devices available on the market.[31a] In an attempt to identify the key physical determinants influencing embolic particle flow in a physiological scenario, we have adopted a simplistic approach and isolated individual forces acting on a single flowing spherical particle (**Table 5**). The combined action of these forces will determine the spatial partitioning of particles at branching sites within the vascular system, and therefore the location of the primary vascular occlusion sites. It should be noted that the relative direction of action of these forces may depend upon the specific architecture of the target vasculature, making it difficult to draw generalized conclusions on the directionality of the net force. For simplicity, we herein consider the case of a steady flow of an embolic particle in a planar vascular network, which lays in a plane perpendicular to the direction of gravity.

It appears evident from Table 5 that it is the interplay between numerous physical parameters which determines the flow behavior of embolic particles in the bloodstream. Parameters include those associated with the carrier fluid (i.e., local blood density, dynamic viscosity, velocity), the vessel in which particles are flowing (i.e., hydraulic diameter and radius of curvature), and the embolic device (size, position within the vessel, compressibility, density, velocity). Blood physical properties will in turn depend on the local hematocrit, and therefore on red blood cell distribution across the vascular system. Vessel distensibility has not been considered in this simplified description, however it may significantly affect the flow behavior of particles and blood cells, particularly when pressure fluctuations originate from embolic events.

A faithful replication of these physical variables represents a considerable experimental challenge, and current models are able to mimic only a limited range of the physical determinants influencing embolization performance. For instance, given the difficulty in systematically controlling and predicting the local hemodynamic profile and architecture of a patient-specific vascular bed, previous studies have focused predominately on the effect of particle physical properties as a determinant of spatial distribution and embolization performance. Furthermore, in order to overcome the economical, ethical, and technical issues associated with the use of animal models in research, efforts have been recently focused on developing artificial models capable of providing measurable performance indicators for comparison between different embolic agents. These models may be designed to reproduce either quantitative or qualitative features of the physiological target vasculature, and are usually tailored to study the effect of a specific set of properties of the embolic devices under investigation.

4.2. Evaluating Embolic Penetration and Migration

An experimental apparatus has been developed by Lewis et al. to study the migration and occlusion performance of drug-loaded hydrogel microspheres in a 2D environment.[21] It consisted of a high aspect ratio, tapered channel whose height varied linearly from 555 to 25 µm. Microspheres were introduced into the flow of a carrier fluid (i.e., saline solution), and a constant static pressure at the inlet boundary of 40 mmHg was imposed to emulate blood pressure in vessels of comparable size (**Figure 8**). Microspheres migrated into the channel

© 2017 WILEY-VCH Verlag GmbH & Co. KGaA, Weinheim

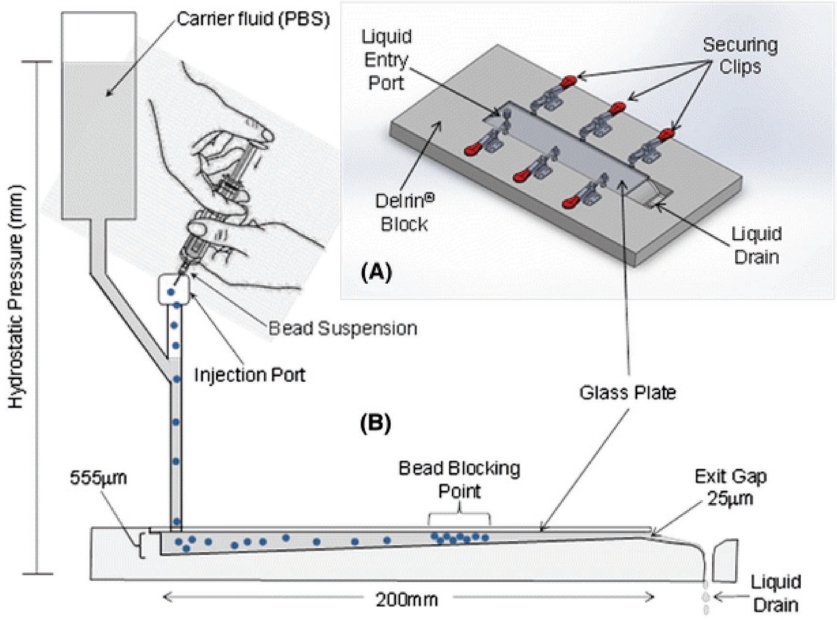

Figure 8. Schematic of the 2D microsphere penetration model. Microspheres were introduced at the wide end of a tapered chamber into a constant flow of a carrier fluid, and migrated into the chamber until they were physically constrained by their size and could not translate more distally (microsphere blocking point). Reproduced with permission.[21] Copyright 2016, Springer.

until they were physically constrained by their size and could not penetrate more distally. Using this apparatus, the penetration distance of microspheres with different size was investigated, and smaller microspheres (diameter range 70–150 µm) were observed to migrate more distally compared to the larger sizes (100–300, 300–500, and 500–700 µm). Furthermore, a direct correlation between microsphere size dispersity and repeatability of the penetration performance was observed, suggesting that a narrower size distribution may lead to consistent positioning of the embolic sites. This model significantly simplifies the physiological environment, as the geometrical constraints are such that microspheres flow is purely dominated by Stokes drag. However, it provides a useful investigational tool for assessing the effect of microsphere size and compressibility on the penetration performance.

4.3. Vascular Models of Embolization

In an attempt to develop a physiologically relevant vascular model,[71] Jernigan et al. constructed an artificial surrogate of the liver tumor vasculature which comprised of 64 silicon tapered microchannels arrayed between two glass plates. Channel width varied from 15.6 µm (inlet) to 20 700 µm (outlet), while channel height varied from 500 µm (inlet) to 32 µm (outlet). This resulted in mean fluid velocities comparable to those observed in arterioles. The model was connected to a pressurized surrogate arterial system for administration of glass or resin embolic microspheres under varying flow rates, and could be rotated for investigating gravitational effects on microspheres. As for the single-channel tapered model presented by Lewis et al., a Newtonian carrier fluid was employed although its dynamic viscosity was adjusted so as to mimic the bulk physical properties of blood. Using this model, authors observed that resin microspheres penetrated more distally compared to glass microspheres, which was attributed to the higher Stokes drag force experienced by the larger resin microspheres. Glass microspheres were instead more sensitive to variations in the inclination angle, given the higher density contrast compared to the surrounding carrier fluid. The authors however, concluded that drag force was the major determinant of microsphere penetration in their model. Despite combining the effect of drag and gravitational forces on a single experimental platform; this model does not replicate the geometrical features of vascular systems, particularly in terms of channel cross-sectional shape, length, and presence of branching structures. Furthermore, channel size relative to microsphere diameter was such that only a minor embolic effect could be generated in this system.

In order to more closely replicate the architecture of vascular networks and related microsphere injection protocols, Richards et al. developed a model of the proximal hepatic circulation using tubes of varying diameter (in the range 6.00–2.68 mm) made of transparent urethane resin (**Figure 9**).[58b] The model comprised of one inlet and five daughter channels, and was employed to investigate the spatial distribution of polypropylene microspheres ranging in size from 106 to 125 µm with densities of 0.9–1.1 g cm^{-3}. It allowed control of the radial injection site and investigation of the effect on particle distribution. Using this system, authors demonstrated potential for achieving individual branch targeting by controlling the particle injection location, and this was further validated using a computational fluid dynamic (CFD) model. Studies were conducted using a Newtonian fluid replicating bulk density and viscosity of blood, which was injected at a constant flow rate (corresponding to an inlet Reynolds number of 600–700). Despite its utility in evaluating clinical injection procedures and their effect on particle distribution, this apparatus is not intended to model confinement or embolic effects that occur during clinical treatment.

Further CFD investigations have been performed on a similar model of the hepatic arterial circulation by Basciano et al.[72] The flow behavior of radiolabeled microparticles of different densities (SIR-Sphere and TheraSpheres) was simulated by imposing a physiologically relevant pressure wave at the inlet boundary. Using this model, the temporal dynamics of particle injection was found to have a significant influence on downstream particle behavior. Specifically, the accelerating phase of the inflow waveform was observed to cause minimal radial particle dispersion, resulting in negligible effects of particle diameter and density. The reduced velocity during the decelerating phase of the waveform however resulted in particle trajectories being dominated by their physical properties (i.e., density). As

© 2017 WILEY-VCH Verlag GmbH & Co. KGaA, Weinheim

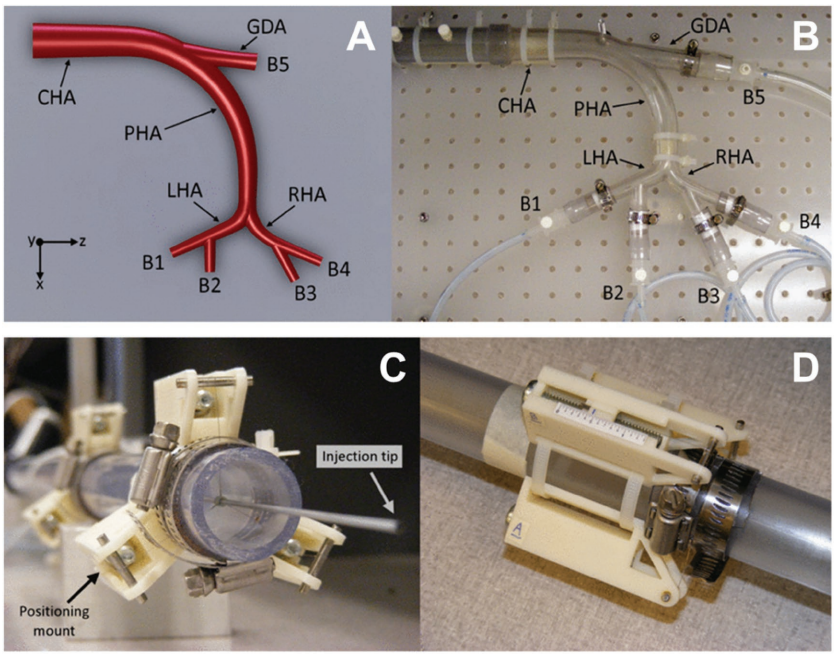

Figure 9. Hepatic artery model to study injection and distribution of embolic particles. A) Schematic of the model geometry and B) photograph of the experimental setup (acquired at 4.4× magnification). C,D) Injection tip positioning system. Reproduced with permission.[58b] Copyright 2012, IEEE.

for previous studies, embolization dynamics was not investigated using this model.

A planar model of the human liver vasculature was also recently developed by Xu et al.[73] to study quantitative endpoints during embolization. Channel diameter ranged from 6 mm (celiac artery) down to 1 mm arterial branches, and physiological values of static pressure (70–150 mmHg) and flow rate (200–500 mL min^{-1} through the whole liver) were replicated using a homogeneous non-Newtonian fluid. Pinch valves were employed to block the flow through selected vascular branches and investigate particle flow postembolization. The model was validated using numerical simulations, and used to investigate particle flow dynamics before and after deployment of an antireflux, conical tip catheter. A relationship between pressure drop across the deployed catheter tip and level of embolization was determined, which could be used clinically to identify the optimal infusion stop point. In its configuration, however, the model did not allow for a faithful dynamic replication of the different phases of the embolization process.

In order to enable detection of microspheres flow pre-, during, and postembolization, Caine et al. developed a silicon-based vascular flow simulator (VFS) representative of a first-order hepatic bifurcation, with channel diameter ranging from 4 mm (proximal) to 0.9 mm (distal) (**Figure 10**).[74] The model allowed for in situ monitoring of microspheres spatial distribution and high-throughput screening of different embolic agents, where microsphere flow depends on the combined effect of viscous, inertial (shear-gradient lift), and gravitational forces. Moreover, it contained meshed filter manifolds to generate embolic flow restrictions and evaluate their effect on microsphere spatial distribution. This also allowed visualization of retrograde flow postembolization, which could be characterized in terms of relative injection velocity or administration style. Notably, the vascular model was integrated with fluid pumping units, making the platform suitable for clinical training purposes. Microsphere-induced embolization could be generated and visualized using this model, making it suitable for comparative analyses between different embolic devices or clinical injection procedures.[75] Recently, the authors have presented a method incorporating the VFS geometry in a quantitative function to analyze the distribution of radioembolic microspheres. It was found that the pulsatile flow system combined with a single-order bifurcating geometry was sufficient to investigate material density and the presence of gravitational effects.[76]

4.4. Microfluidic Models of Embolization

With the aim of revealing and quantifying the complex phenomenology of embolization processes, Carugo et al. developed a microfluidic-based model of the tumor microvasculature comprising of a 1000 µm diameter feeding channel and four outlet channels (minimum diameter = 200 µm) (**Figure 11**).[77] The model was fabricated in a layer of highly transparent poly(methyl-methacrylate) (PMMA) via micromilling technology. The device could thus be coupled with an optical microscope for direct observation of microspheres distribution and embolization dynamics. Notably, both single- and multi-microsphere embolic modalities could be generated by injecting a suspension of microspherical PVA microspheres (Bead Block) with diameter ranging between 300 and 900 µm (Figure 11B,C), in a continuous flow of a Newtonian fluid (inlet Reynolds number = 3.6–72.2). A penetration efficacy coefficient was introduced to quantify the ability of a given microsphere suspension to penetrate distally within a vascular network. Notably, given the smaller channel dimension compared to other models, the flow behavior of embolic microspheres was affected by inertial forces arising from microsphere confinement (wall interaction lift), in addition to viscous, gravitational, and shear-gradient lift forces. The effect of confinement was evident when microspheres of different size were compared in terms of their partitioning at bifurcations. The model however replicated only a limited segment of the distal tumor vasculature, therefore it could not be used for injection of a therapeutically relevant amount of embolic material or for replicating clinical injection modalities, as for the larger model systems (i.e., VFS).

Using the same platform, the authors revealed for the first time the flow dynamics in embolized microvessels, which was characterized by the presence of residual flow postembolization and the formation of laminar vortices within the cavity formed by the vascular occlusion (Figure 11D).[78] However, the physical properties of both fluids and microchannels did not replicate

© 2017 WILEY-VCH Verlag GmbH & Co. KGaA, Weinheim

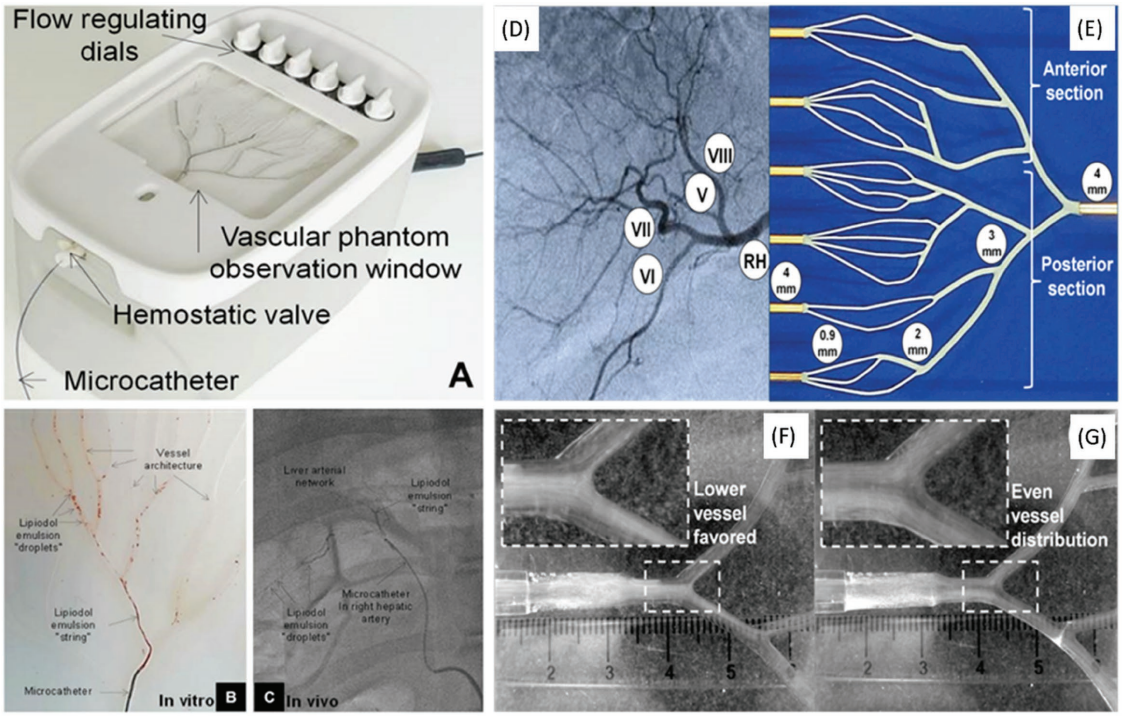

Figure 10. A) Vascular flow simulator (VFS) for evaluation of embolic agent delivery, highlighting effects of administration parameters; B) photograph of the vascular phantom during delivery of a Lipiodol tracer; C) visual similarities in emulsion appearance on fluoroscopy during in vivo administration. D,E) Typical vascular anatomy and schematic of vascular network, respectively. F,G) High-speed video still of microsphere distribution under flow, favoring upper and lower flow channels in vertical device orientation. Reproduced with permission.[74] Copyright 2015. Reproduced with permission.[76] Copyright 2016, Elsevier.

those of a physiological system, and may have impacted on the experimental observations.

Despite the challenges associated with modeling of vascular structures, efforts have been made in an attempt to develop investigational platforms to study flow behavior and occlusion performance of embolic particles. These platforms are usually designed to replicate some of the physical determinants of embolization, so as to resolve specific differences between embolic devices or clinical procedures. While recent advances in technology (i.e., rapid prototyping) may open the way for the development of patient-specific models, simplified mimics of the target vasculature are often preferred as they provide measurable indicators of performance which are easier to interpret. However, these modeling simplifications may have impeded a quantitative correlation between in vitro and in vivo correlation (IVIVC). Qualitative agreement has been however demonstrated in some cases; for instance, segmental analysis of various embolic particles in a rabbit kidney embolization model have supported the 2D penetration information provided by the tapered channel model, if a radial correction factor is applied.[21] The spatial distribution of microspheres injected in the VFS model following a clinical administration procedure closely replicated spatial distribution patterns observed in vivo.[74] Furthermore, phenomenological observations obtained using the microfluidic-based arteriolar model qualitatively agreed with previous animal studies.[74]

Future developments to current model systems may be required to achieve quantitative IVIVC, as follows:

(i) Models usually replicate either a proximal or distal segment of the target vasculature. Proximal models are suitable for investigating spatial distribution of particles and its dependence on injection procedures, while distal models can be employed to study embolic events and their spatiotemporal dynamics. A system capable of integrating proximal and distal vascular segments in a single platform will allow a direct correlation between clinical administration procedures, hemodynamic boundary conditions, and embolization endpoints.

(ii) Fabrication of such a model represents a technological challenge, given the large variation in vessel dimension along the vascular tree, that is, from few millimeters (proximal) to tens of micrometers (distal). Moreover, given the clinical tendency for reducing the size of embolic particles, microfabrication technologies may be required in order to generate channels suitable for embolic endpoints.

(iii) Current models do not faithfully replicate the mechanical properties of the vessel wall. Future efforts should be focusing on mimicking those properties, as they may significantly impact on embolization dynamics.

(iv) Previous studies have demonstrated that microsphere injection (i.e., radial position) has a significant impact on microsphere spatial distribution, however only few models replicated clinical procedures of injection. This is an important prerequisite, as it may allow development and validation of clinical recommendations for embolics administration. Specific focus on the rate of injection in

© 2017 WILEY-VCH Verlag GmbH & Co. KGaA, Weinheim

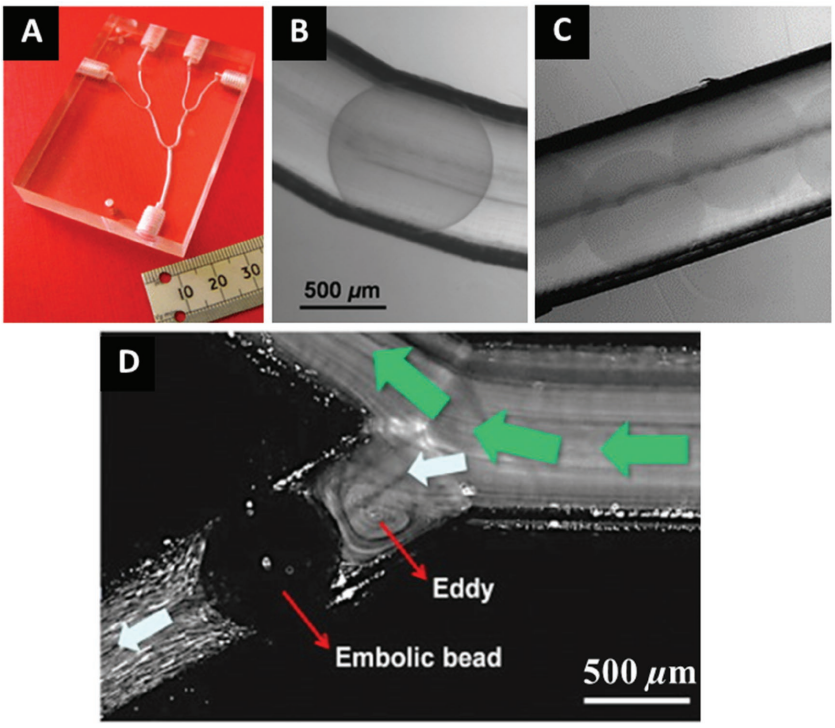

Figure 11. A) Photograph of the microfluidic-based microchannel network device for embolization studies. B,C) Microscope images of single- and multi-microsphere embolization achieved within the device. Reproduced with permission.[77] Copyright 2012, Springer. D) Microscope image of fluorescent tracer particles flowing within the microfluidic device, in close proximity to a single-microsphere embolic event. Green arrows indicate the systemic flow direction, while light blue arrows indicate the presence of residual fluid flow rate in the embolized channel. Formation of laminar vortices within the embolized channel, in close proximity to the embolic microsphere, is clearly detectable. Reproduced with permission.[78] Copyright 2015, Elsevier.

combination with the embolic concentration should also be considered.

(v) The large majority of studies have been conducted utilizing Newtonian blood surrogates as carrier fluids. Future studies should be performed using biological fluids (i.e., full blood or diluted suspensions of blood cells), given that blood constituents may profoundly influence the fluid dynamic field both pre- and postembolization, and also closely interact with the embolic material. Furthermore, attention must be paid to the replication of clinical procedures of particle resuspension prior to administration (i.e., using contrast agents).

(vi) A quantitative validation of embolization models requires the ability to detect and quantity performance indicators, via integration with analytical methods. These may include flow and pressure sensing units to monitor hemodynamic parameters at different temporal stages of the embolization process (i.e., from injection to vascular occlusion), optical detection, and image analysis techniques to track particle distribution and quantify the spatial position of embolization endpoints, and flow visualization techniques to determine local fluid dynamic events including presence/absence of residual flow postembolization, flow patterns in occluded branches, and retrograde flow postembolization.

5. Microsphere Drug Elution Studies

As for any product containing a pharmaceutical active, before any DEB can be evaluated in men it is necessary to gain an understanding of how the loaded drug will elute in the body.[79] When administered, DEBs first travel through the blood, carried by the flow within the vessel. At this stage, DEBs are bathed in an ion-rich medium that can initiate the ion-exchanged and drug release process. This is only the case for a few moments however, as blood flow is reduced by the DEB becoming lodged within the vessel lumen and may reach complete stasis dependent upon the amount of DEB injected (steps D and E in Figure 5). The stagnation of flow will cause blood to clot around the microspheres and drug release is then a function of ion diffusion into, and drug diffusion out of the DEB and into the surrounding tissue milieu.

5.1. Evaluation of Microsphere–Drug Interaction

The mechanism of ion-exchange for DC Bead has been studied in detail using a variety of experimental evaluations and mathematical modeling.[80] Drug and water distribution and their transport phenomena within the microsphere structure have provided some mechanistic insight into drug–microsphere interactions.[80a] Isothermal titration calorimetry has been investigated for its suitability in determining stoichiometry and thermodynamics of drug–bead interactions.[81] Drug elution investigations at the single microsphere level have also been performed using a microfluidic device consisting of a network of microchannels. The spatiotemporal dynamics of doxorubicin elution from DC Bead was determined using bespoke microscopic and spectrofluorometric methods.[78a] Confocal laser scanning microscopy (CLSM) is particularly useful for evaluating the presence and distribution of fluorescent drugs such as doxorubicin inside the bead structures, although quenching effects at high drug concentration can create artifacts.[33] Fluorescent recovery after photobleaching (FRAP) and fluorescence correlation spectroscopy (FCS) can be used to overcome these issues and reveal information on drug transport properties through the hydrogel matrix.[80] Fourier transform infrared (FTIR) microscopy can also be used to create an image of drug distribution through bead sectioned using a microtome.[82] A calibration curve can be constructed using beads with different drug loadings and this used to estimate the amount of drug left residing in beads embedded within histological sections from explanted tissue specimens.[83] Furthermore, FTIR can

© 2017 WILEY-VCH Verlag GmbH & Co. KGaA, Weinheim

also be used to demonstrate specific interactions between drug and chemical functions within the beads, as there are subtle changes in the stretching frequency of the moieties that interact with the drug by ion-exchange, which correlate with concentration of drug bound to these groups.[84] These methods provide detailed behavioral information on the micrometer level but do not predict the outcome for locoregional delivery from an embolic mass, for which elution methods capable of assessing release from a physiologically relevant volume of microspheres are necessary.

5.2. Microsphere Elution Methods

Intra-arterial drug delivery is a complex scenario to model in vitro and while standard USP type 1–6 apparatus that are used to evaluate tablet dissolution have been adapted to demonstrate the relative rates and total extent of release of drug from beads (**Figure 12**), they have little bearing on how drug is released within the body.[79a] A T-apparatus method has been described by Amyot et al.[85] which attempted to incorporate a drug diffusion and convection zone to emulate drug release into the embolized regions and its eventual extraction from the tissue by blood flow in distant vessels.[86] The depth of the well in which the microspheres sit within the apparatus can be varied to alter the diffusion distance and hence vary the apparent rate of elution.[86] This has been used successfully in a number of reported studies and good in vitro in vivo correlation has been shown with drug plasma levels over the first 24 h post DEB treatment.[35c,79a]

This model is however, not without practical difficulties and others have adopted the USP IV flow-through apparatus as a more rapid and reproducible model for microsphere elution (Figure 12).[32a,52b,87] This method, however, also suffers from limitations as some products have been shown to lose mass due to the rate of flow of the eluent through the microsphere mass and incomplete drug release has also been reported, which is an artifact of the method rather than a property of the DEB under study.[32a,87c] Others have described the use of two miniaturized in vitro methods based upon a free-flowing or sample reservoir setup that allows release rates to be measured under different conditions with reduced amounts of sample, release medium, and waste.[88] They proposed the low volume of in vitro release medium used may better correlate to the in vivo situation due to the low availability of releasing medium at the target site.[88,89] Recently, a modified flow-through method has been described that uses an occluded mass of microspheres to emulate the embolization and can be adapted to take into account dimensional changes in the microspheres during elution.[90] Whereas burst release of drug into the blood is dependent upon microsphere size (surface area to volume), and administration rate in terms of absolute concentration of exposed drug

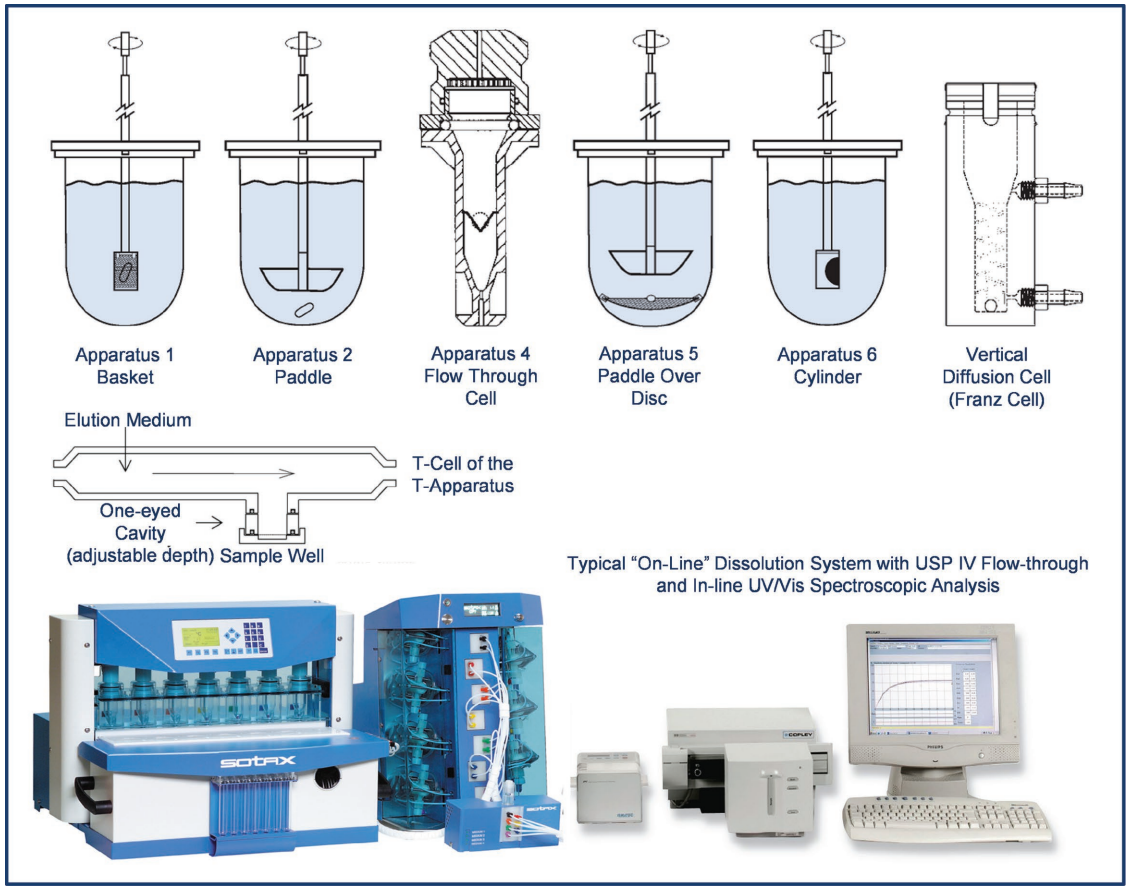

Figure 12. Schematic of various USP drug elution apparatuses and a T-cell elution setup, and photograph of an in-line dissolution system.

© 2017 WILEY-VCH Verlag GmbH & Co. KGaA, Weinheim

containing microspheres, once in an occluded mass the elution is dependent largely on the concentration of ions present (or rate at which they flow through the system) and this method has been shown to be predictive of in vivo drug release.[90] The specific elution kinetics pertaining to the early phase of administration (which is typically associated with highest plasma profiles in pharmacokinetic studies) are currently under investigation using a modification of the vascular flow system shown in Figure 10.

5.3. In Vitro Cell Culture Methods for Evaluating Microsphere Efficacy

Cell viability assays have been used in which DEBs loaded with one or a combination of drugs are placed in wells and the effect of the drug eluting into the media on cell survival is measured over time.[91] These studies provide some confidence that the drug can be released over time in a biological medium and has the desired effect on the cells. The effects of hypoxia have also been studied using in situ–in vitro PK/PD models,[92] and this combined with studies on DEB exposure to cells in various flow conditions and drug types[87a,92c] has the potential to provide the missing biological element to in vitro testing. Excellent advances have been made in testing implanted cells for various organs in response to drug compounds,[93] however little work has been performed to integrate this biomolecular interaction with scaled physical conditions associated with embolic delivery. Although many in vitro methods exist for evaluation of embolic agents, there is still a fundamental requirement for biological testing. This may come in the form of immunohistocompatibility, tumor kill ratios, or cascade reactions that are currently too complex and multifaceted to be effectively modeled in vitro.[94] Vasculature-on-a-chip models may however provide an experimental platform for investigating the effect of beads physical properties and flow behavior on biological effects.

5.4. Spectroscopic Methods for In Vivo Drug Delivery Evaluations

In vitro modeling can only provide guidance information and ultimately plasma pharmacokinetic studies provide the best estimate of drug release into the systemic circulation post DEB administration, and hence an estimate of the likelihood of drug-related adverse side effects. Of more interest is the accumulation of drug into the target tissue over time. For doxorubicin, which is highly fluorescent, this has been studied using epifluorescence microscopy[29] or microspectrofluorimetry[83] on histological sections of tissues containing microspheres. Sunitinib is also fluorescent and its distribution in tissue has been studied by fluorescence microscopy and compared to that measured by Matrix-assisted laser desorption/ionization-selected reaction monitoring/ mass spectrometry (MALDI-SRM/MS) imaging.[95] Moreover, DEBs containing ibuprofen, doxorubicin, and irinotecan have been assessed in various in vivo embolization models and residual drug remaining within the microspheres at certain time points postdelivery has been quantified using techniques such as infrared microspectroscopy.[82b,83] A large amount of drug is released into the surrounding tissues within the first hours and can diffuse several hundred micrometers from the DEB surface.[29,83,96] More drug is released further from clusters of microspheres compared to single microspheres as they act as a giant reservoir for drug. In several studies, it has been shown in animal models around 70% of the loaded dose is released within the first week and 90%–100% within a month.[29,83] It has been suggested that there may be a tissue dose maximum whereby the rate of doxorubicin release into the tissue is governed by diffusion and local ion concentration rather than DEB release properties, higher doses rather serving to extend the period over which the drug is released. Tissue mimic models are currently being investigated for their use in confined elution profiling of drug-loaded microspheres. The alignment of diffusion distance as a function of time with that of previous histological analyses will enable a fast and simple profiling tool for measuring a variety of features such as packing volume, novel chemistries, and the effect of external physical stimuli, such as ultrasound, on modified elution kinetics.

6. Perspectives on Regulation for the Development of Microspheres for Embolotherapy

Particulates or microspheres that are intended for use as artificial emboli and that are permanent in nature are classed as medical devices artificial embolization device (AED). They are regulated in the EU as a Class IIB—in case of bland embolization—under medical device directive MDD 93/42/EEC and in the United States as a Class II vascular and neurovascular embolization device, as their primary mode of action (PMOA) is that of physical occlusion of a vessel. Since PVA particles have been used for the indication of general embolization of vessels for over 40 years, they provide a comparative device against which subsequent next generation products have gained approval or clearance for use based upon substantial equivalence. Some of the test methods described in this review therefore, have evolved as a consequence of manufacturers' requiring comparative bench data to demonstrate the performance characteristics of their products similar to appropriate equivalent products.

With the addition of new features to the embolic devices comes the necessity for additional burden of proof, to demonstrate continued safety of the device and an appropriate risk–benefit profile for the new product. Naturally, devices composed of new materials hitherto untested for implantation require a complete evaluation of biocompatibility and toxicity, generally according to the testing regimes described in the International Standard ISO10993-1 "Biological evaluation of medical devices – Part 1: Evaluation and testing within a risk management process" (FDA guidance issued June 16 2016). There may also be a necessity for clinical data in certain instances. Simple line extensions, such as additional size ranges, for instance, can be approved by supplements to the design dossier for CE mark or additional 510(k) applications with appropriate evidence that the changes raise no additional safety concerns and the device remains effective in its intended use.[21] The addition of

© 2017 WILEY-VCH Verlag GmbH & Co. KGaA, Weinheim

radiopacity to the device introduces the new capability to visualize the location of the microspheres intra and postprocedurally in order to better target their application and would require a new product application.[22] In addition to the considerations around new materials, there must be demonstration that the addition of the radiopacity does not adversely alter other properties of the microspheres, and that the device can still be handled and administered easily for use in the Cathlab. This requires a deep appreciation of the way in which the physicians use the products in clinical practice and guidance is provided by regulators to help device comprehensive usability and human factor studies for relevant "use" testing ("Applying Human Factors and Usability Engineering to Medical Devices," FDA guidance issued February 3 2016 and BS EN 62366:2008+A1:2015, "Applicability of Usability Engineering to Medical Devices"). The regulatory perspective on the feature of biodegradability/bioresorption of a device is more complex and may also relate to the rate at which the device is broken down in the body. There is obviously a requirement to understand and demonstrate what the materials of the device are broken down into and how these are ultimately excreted from the body. This can be a significant undertaking with radiolabeling studies recommended to trace the fate of the breakdown products in the body as they are eliminated.[97] This undertaking can be too high a hurdle for some manufacturers with limited resources and many opt to use materials such as polylactide/glycolide (co)polymers as the basis of their devices as the breakdown products and pathway of elimination are well known to the regulators and require less evidence. This does, of course, have the effect of stifling innovation of novel products. An example is the Occlusin 500 Biodegradable Embolic Microsphere,[20c] which was cleared by FDA in December 2009 based on a 510(k) application of substantial equivalence to the EmboSphere (nondegradable) Embolic Microsphere. As Occlusin 500 materials of composition are well known (poly(lactic-*co*-glycolic acid) coated with bovine collagen) and the degradation rate slow (>3 months) this product was deemed safe and substantially equivalent to a nondegradable predicate device.

When considering the combination of the embolization microsphere with a drug, as in the case of DEBs, the regulatory viewpoint changes and an algorithm is employed in order to determine the PMOA. The intention of the device component is still physical occlusion of the blood vessel, whereas the drug component is to be released locally in order to have a specific pharmacological action and biological effect, for example, an antitumoral effect. The FDA recognized that combination products (any combination of a drug, device, or biologic in a product at the point of use in a patient)[98] were evolving in complexity and introduced the Office of Combination Products (OCP) to address these issues. A request for designation (RFD) procedure was introduced that allows manufacturers to submit a description of their proposed combination product to OCP in order to initiate discussions around its assignment as primarily either drug, device, or biologic. FDA also recognized the challenges in the manufacture of such products given that different standards could be applied depending upon the view on the PMOA of the product and have provided guidance (Guidance for Industry and FDA Staff: Current Manufacturing Practice Requirements for Combination Products, draft guidance issued January 2015). For the European regulatory situation, DEBs with the primary mode of action being the occlusion of the blood vessels and the intention to delivery medicines loaded by the physician into the microspheres are seen as Class III products. Preloaded microspheres do include a medicinal product as an integral component and thereby are regulated as combination products. The presence of the drug, however, may alter the risk–benefit profile of the product and the level of clinical evidence required to gain regulatory approvals for these types of combination products can be both very extensive and costly for the manufacturers.

7. Summary

The present review of embolic microspheres provides an overview of the main considerations involved in their development, preparation through to final administration in patients, and the various tools and techniques that have been applied in their characterization in order to gain an appreciation of their performance and behavior. In doing so, we highlight certain elements that could warrant further examination in order to improve our fundamental understanding of the unique physical properties of this highly dynamic clinical procedure.

Clearly there is a need for more bespoke tests that help better predict clinical performance and will enable reduction in unnecessary animal testing, in conformance with the principles of the 3R's. An area lacking detailed study is that of the flow mechanics experienced during administration, and modeling of the directionality and end location of the devices under standardized administration parameters. This would improve our understanding of the procedural variables, distribution of the embolic devices within the vasculature, endpoint effects, and many other factors that influence the overall effectiveness of the treatment.

For DEBs there is still a lack of a drug elution test method that adequately predicts drug diffusion in embolized tumors. There are multiple methods available and it may be that a combination of different methods is required to gain a full appreciation of the early, mid and late phases of drug release from point of administration through to many months postembolization. Indeed, the early stages of drug elution occur as the DEB is being delivered and in-transit through the blood vessels; a stage of release not currently accounted for in current methods yet could be the single most important event for determining peak plasma drug concentrations and hence drug-related adverse events in patients.

Embolic microspheres continue to evolve with clinical practice, with additional features being designed into the devices to provide added functionality for the user, such as imaging capability so that the location of the devices can be tracked intra and postprocedurally. Each added function will require a test method to measure, monitor, and predict performance and long-term safety of the device in the body. Henceforth, test method development itself will require parallel evolution in compliance with the principles of the 3R's, to remain ethical, moral, and relevant to clinical practice.

Received: November 17, 2016
Revised: January 4, 2017
Published online:

© 2017 WILEY-VCH Verlag GmbH & Co. KGaA, Weinheim

[1] K. M. Z. Hossain, U. Patel, I. Ahmend, *Prog. Biomater.* **2015**, *4*, 1.
[2] a) K. H. Ramteke, V. B. Jadhav, S. N. Dhole, *IOSR J. Pharm.* **2012**, *2*, 44; b) V. V. Prasanth, A. C. Moy, S. T. Mathew, R. Mathapan, *Int. J. Pharm. Biomed. Sci.* **2011**, *2*, 332.
[3] K. Kyyronen, L. Hume, C. Benedict, A. Urtti, E. Topp, V. Stell, *Int. J. Pharm.* **1992**, *49*, 732.
[4] N. F. Farraj, B. R. Johansen, S. S. Davis, L. Illum, *J. Controlled Release* **1990**, *80*, 161.
[5] S. Geary, S. W. Schalamens, *J. Controlled Release* **1993**, *46*, 661.
[6] a) P. Chandrawanshi, H. Patidar, *J. Pharm. Res.* **2009**, *2*, 964; b) S. Kakar, D. Batra, R. Singh, U. Nautiyal, *J. Acute Dis.* **2013**, *2*, 1.
[7] a) U. K. Kotreka, M. C. Adeyeye, *Crit. Rev. Ther. Drug Carrier Syst.* **2011**, *28*, 47; b) D. Sathish, S. Himabindu, Y. S. Kumar, Shayeda, Y. M. Rao, *Curr. Drug Delivery* **2011**, *8*, 494.
[8] a) E. W. Lee, L. Alanis, S. K. Cho, S. Saab, *Korean J. Radiol.* **2016**, *17*, 472; b) N. Khajornjiraphan, N. A. Thu, P. K. Chow, *Liver Cancer* **2015**, *4*, 6.
[9] a) A. Kiani, N. J. Lakhkar, V. Salih, M. E. Smith, J. V. Hanna, R. J. Newport, D. M. Pickup, J. C. Knowles, *Philos. Trans. R. Soc., A* **2012**, *370*, 1352; b) N. J. Lakhkar, J. H. Park, N. J. Mordan, V. Salih, I. B. Wall, H. W. Kim, S. P. King, J. V. Hanna, R. A. Martin, O. Addison, J. F. Mosselmans, J. C. Knowles, *Acta Biomater.* **2012**, *8*, 4181.
[10] N. K. Varde, D. W. Pack, *Expert Opin. Biol. Ther.* **2004**, *4*, 35.
[11] K. Saralidze, L. H. Koole, M. L. W. Knetsch, *Materials* **2010**, *3*, 3537.
[12] J. J. Blaker, J. Pratten, D. Ready, J. C. Knowles, A. Forbes, R. M. Day, *Aliment. Pharmacol. Ther.* **2008**, *28*, 614.
[13] P. Landwehr, S. Arnold, G. Voshage, P. Reimer, *Der Radiol.* **2008**, *48*, 73.
[14] S. Vaidya, K. R. Tozer, J. Chen, *Semin. Interv. Radiol.* **2008**, *25*, 204.
[15] a) M. Herrera, J. Rysavy, F. Kotula, B. Rusnak, W. R. Castaneda-Zuniga, K. Amplatz, *Radiology* **1982**, *144*, 638; b) S. M. Tadvarthy, J. H. Moller, K. Amplatz, *Ther. Nucl. Med.* **1974**, *125*, 609.
[16] a) S. Muppalaneni, H. Omidian, *J. Dev. Drugs* **2013**, *2*, 112; b) G. S. Davidson, K. G. Terbrugge, *AJNR* **1995**, *16*, 843.
[17] C. P. Derdeyn, C. J. Moran, D. T. Cross, H. H. Dietrich, R. G. Dacey Jr., *AJNR* **1995**, *16*, 1335.
[18] a) R. Beaujeux, A. Laurent, M. Wassef, A. Casasco, Y. P. Gobin, A. Aymard, D. Rufenacht, J. J. Merland, *AJNR* **1996**, *17*, 541; b) A. Laurent, R. Beaujeux, M. Wassef, D. Rufenacht, E. Boschetti, J. J. Merland, *AJNR* **1996**, *17*, 533.
[19] a) P. Giunchedi, M. Maestri, E. Gavini, P. Dionigi, G. Rassu, *Expert Opin. Drug Delivery* **2013**, *10*, 679; b) P. Giunchedi, M. Maestri, E. Gavini, P. Dionigi, G. Rassu, *Expert Opin. Drug Delivery* **2013**, *10*, 799.
[20] a) L. Weng, P. Rostamzadeh, N. Nooryshokry, H. C. Le, J. Golzarian, *Acta Biomater.* **2013**, *9*, 6823; b) L. Weng, M. Rusten, R. Talaie, M. Hairani, N. K. Rosener, J. Golzarian, *JVIR* **2013**, *24*, 1567; c) R. J. Owen, P. N. Nation, R. Polakowski, J. A. Biliske, P. B. Tiege, I. J. Griffith, *CVIR* **2012**, *35*, 636.
[21] A. L. Lewis, M. R. Dreher, V. O'Byrne, D. Grey, M. Caine, A. Dunn, Y. Tang, B. Hall, K. D. Fowers, C. G. Johnson, *J. Mater. Sci.: Mater. Med.* **2016**, *27*, 1.
[22] a) R. Duran, K. Sharma, M. R. Dreher, K. Ashrafi, S. Mirpour, M. Lin, R. E. Schernthaner, T. R. Schlachter, V. Tacher, A. L. Lewis, S. Willis, M. den Hartog, A. Radaelli, A. H. Negussie, B. J. Wood, J. F. Geschwind, *Theranostics* **2016**, *6*, 28; b) E. B. Levy, V. P. Krishnasamy, A. L. Lewis, S. Willis, C. Macfarlane, V. Anderson, I. M. van der Bom, A. Radaelli, M. R. Dreher, K. V. Sharma, A. Negussie, A. S. Mikhail, J. F. Geschwind, B. J. Wood, *CVIR* **2016**, *39*, 1177; c) K. V. Sharma, Z. Bascal, H. Kilpatrick, K. Ashrafi, S. L. Willis, M. R. Dreher, A. L. Lewis, *Biomaterials* **2016**, *103*, 293.
[23] a) C. W. Kerber, W. O. Bank, J. A. Horton, *AJR, Am. J. Roentgenol.* **1978**, *130*, 1193; b) M. Lubarsky, C. Ray, B. Funaki, *Semin. Interv. Radiol.* **2010**, *27*, 99.
[24] a) A. Laurent, M. Wassef, J. P. Saint Maurice, J. Namur, J. P. Pelage, A. Seron, R. Chapot, J. J. Merland, *Invest. Radiol.* **2006**, *41*, 8; b) J. P. Pelage, A. Laurent, M. Wassef, M. Bonneau, D. Germain, R. Rymer, P. Flaud, J. Martal, J. J. Merland, *Radiology* **2002**, *224*, 436.
[25] R. Bandi, P. C. Shetty, R. P. Sharma, T. H. Burke, M. W. Burke, D. Kastan, *JVIR* **2001**, *12*, 1399.
[26] T. Sorimachi, T. Koike, S. Takeuchi, T. Minakawa, H. Abe, K. Nishimaki, Y. Ito, R. Tanaka, *AJNR* **1999**, *20*, 1323.
[27] a) E. Liapi, K. H. Lee, C. C. Georgiades, K. Hong, J. F. Geschwind, *Tech. Vasc. Interv. Radiol.* **2007**, *10*, 261; b) K. Malagari, *Expert Rev. Anticancer Ther.* **2008**, *8*, 1643; c) A. Nicolini, S. Crespi, L. Martinetti, *Expert Opin. Drug Delivery* **2011**, *8*, 1071.
[28] A. Laurent, E. Velzenberger, M. Wassef, J. P. Pelage, A. L. Lewis, *JVIR* **2008**, *19*, 1733.
[29] M. R. Dreher, K. V. Sharma, D. L. Woods, G. Reddy, Y. Tang, W. F. Pritchard, O. A. Chiesa, J. W. Karanian, J. A. Esparza, D. Donahue, E. B. Levy, S. L. Willis, A. L. Lewis, B. J. Wood, *JVIR* **2012**, *23*, 257.
[30] V. Verret, S. H. Ghegediban, M. Wassef, J. P. Pelage, J. Golzarian, A. Laurent, *JVIR* **2011**, *22*, 220.
[31] a) A. L. Lewis, C. Adams, W. Busby, S. A. Jones, L. C. Wolfenden, S. W. Leppard, R. R. Palmer, S. Small, *J. Mater. Sci.: Mater. Med.* **2006**, *17*, 1193; b) O. S. Sakr, S. Berndt, G. Carpentier, M. Cuendet, O. Jordan, G. Borchard, *J. Controlled Release* **2016**, *224*, 199.
[32] a) O. Jordan, A. Denys, T. De Baere, N. Boulens, E. Doelker, *JVIR* **2010**, *21*, 1084; b) A. L. Lewis, M. V. Gonzalez, A. W. Lloyd, B. Hall, Y. Tang, S. L. Willis, S. W. Leppard, L. C. Wolfenden, R. R. Palmer, P. W. Stratford, *JVIR* **2006**, *17*, 335.
[33] A. L. Lewis, M. V. Gonzalez, S. W. Leppard, J. E. Brown, P. W. Stratford, G. J. Phillips, A. W. Lloyd, *J. Mater. Sci.: Mater. Med.* **2007**, *18*, 1691.
[34] K. Hidaka, M. Nakamura, K. Osuga, H. Miyazaki, S. Wada, *J. Mech. Behav. Biomed. Mater.* **2010**, *3*, 497.
[35] a) R. E. Forster, F. Thurmer, C. Wallrapp, A. W. Lloyd, W. Macfarlane, G. J. Phillips, J. P. Boutrand, A. L. Lewis, *J. Mater. Sci.: Mater. Med.* **2010**, *21*, 2243; b) K. Hidaka, L. Moine, G. Collin, D. Labarre, J. L. Grossiord, N. Huang, K. Osuga, S. Wada, A. Laurent, *J. Mech. Behav. Biomed. Mater.* **2011**, *4*, 2161; c) R. R. Taylor, Y. Tang, M. V. Gonzalez, P. W. Stratford, A. L. Lewis, *Eur. J. Pharm. Sci.* **2007**, *30*, 7; d) R. E. Forster, S. A. Small, Y. Tang, C. L. Heaysman, A. W. Lloyd, W. Macfarlane, G. J. Phillips, M. D. Antonijevic, A. L. Lewis, *J. Mater. Sci.: Mater. Med.* **2010**, *21*, 2683.
[36] a) J. B. Spies, S. Allison, P. Flick, M. Cramp, J. Bruno, R. C. Jha, S. A. Ascher, *JVIR* **2005**, *16*, 1431; b) G. P. Siskin, A. Beck, M. Schuster, K. Mandato, M. Englander, A. Herr, *JVIR* **2008**, *19*, 58.
[37] a) J. E. Dion, R. N. Rankin, F. Vinuela, A. J. Fox, A. C. Wallace, M. Mervart, *Radiology* **1986**, *160*, 717; b) Y. P. Gobin, F. Vinuela, H. V. Vinters, C. Ji, K. Chow, *Radiology* **2000**, *214*, 113.
[38] a) A. J. Greenfield, C. A. Athanasoulis, A. C. Waltman, E. R. LeMoure, *AJR, Am. J. Roentgenol.* **1978**, *131*, 651; b) R. Lencioni, T. Baere, M. Burrel, J. Caridi, J. Lammer, K. Malagari, R. G. Martin, E. O'Grady, M. Real, T. Vogl, A. Watkinson, J.-F. Geschwind, *CVIR* **2012**, *35*, 980.
[39] S. Stampfl, N. Bellemann, U. Stampfl, C. M. Sommer, H. Thierjung, R. Lopez-Benitez, B. Radeleff, I. Berger, G. M. Richter, *JVIR* **2009**, *20*, 1597.
[40] Z. Liu, R. Cheung, X. Y. Wu, J. R. Ballinger, R. Bendayan, A. M. Rauth, *J. Controlled Release* **2001**, *77*, 213.
[41] C. S. Co, N. Yashiro, M. Iio, Y. Mukoyama, *Radiat. Med.* **1983**, *1*, 268.
[42] a) T. Saeki, K. Jinushi, H. Kodama, K. Yoshinaka, T. Toge, M. Niimoto, T. Hattori, *Cancer Chemother.* **1988**, *15*, 2633; b) T. Taguchi, *Cancer Chemother.* **1995**, *22*, 969.
[43] L. Weng, H. C. Le, R. Talaie, J. Golzarian, *JVIR* **2011**, *22*, 1464.

© 2017 WILEY-VCH Verlag GmbH & Co. KGaA, Weinheim

[44] S. Louguet, V. Verret, L. Bedouet, E. Servais, F. Pascale, M. Wassef, D. Labarre, A. Laurent, L. Moine, *Acta Biomater.* **2014**, *10*, 1194.
[45] V. Verret, J. P. Pelage, M. Wassef, S. Louguet, E. Servais, L. Bedouet, T. Beaulieu, L. Moine, A. Laurent, *JVIR* **2014**, *25*, 1759.
[46] a) D. Horak, M. Metalova, F. Rypacek, *J. Biomed. Mater. Res.* **1997**, *34*, 183; b) D. Horak, M. Metalova, F. Svec, J. Drobnik, J. Kalal, M. Borovicka, A. A. Adamyan, O. S. Voronkova, K. Z. Gumargalieva, *Biomaterials* **1987**, *8*, 142; c) D. Horak, F. Svec, J. Kalal, A. Adamyan, N. Skuba, M. Titova, V. Dan, B. Varava, N. Trostenyuk, O. Voronkova, *Biomaterials* **1988**, *9*, 367; d) B. C. Thanoo, A. Jayakrishnan, *J. Microencapsulation* **1989**, *6*, 233; e) B. C. Thanoo, A. Jayakrishnan, *Biomaterials* **1990**, *11*, 477; f) B. C. Thanoo, A. Jayakrishnan, *J. Microencapsulation* **1991**, *8*, 95; g) B. C. Thanoo, M. C. Sunny, A. Jayakrishnan, *J. Appl. Biomater.* **1991**, *2*, 67; h) C. S. van Hooy-Corstjens, K. Saralidze, M. L. Knetsch, P. J. Emans, M. W. de Haan, P. C. Magusin, B. Mezari, L. H. Koole, *Biomacromolecules* **2008**, *9*, 84.
[47] L. S. Peixoto, P. A. Melo, M. Nele, J. C. Pinto, *Macromol. Mater. Eng.* **2009**, *294*, 463.
[48] a) A. H. Negussie, M. R. Dreher, C. G. Johnson, Y. Tang, A. L. Lewis, G. Storm, K. V. Sharma, B. J. Wood, *J. Mater. Sci.: Mater. Med.* **2015**, *26*, 5530; b) K. V. Sharma, M. R. Dreher, Y. Tang, W. Pritchard, O. A. Chiesa, J. Karanian, J. Peregoy, B. Orandi, D. Woods, D. Donahue, J. Esparza, G. Jones, S. L. Willis, A. L. Lewis, B. J. Wood, *JVIR* **2010**, *21*, 865.
[49] a) A. L. Lewis, *Expert Rev. Med. Dev.* **2009**, *6*, 389; b) A. Guibal, T. Lefort, L. Chardon, N. Benslama, S. Mulé, F. Pilleul, C. Lombard-Bohas, L. Bridal, J. Chayvialle, O. Lucidarme, A. Denys, T. Walter, *Eur. Radiol.* **2013**, *23*, 805; c) R. Lencioni, C. Aliberti, T. de Baere, R. Garcia-Monaco, G. Narayanan, E. O'Grady, W. S. Rilling, D. Walker, R. C. G. Martin, *JVIR* **2014**, *25*, 365.
[50] N. Strickland, M. Rampling, P. Dawson, G. Martin, *Clin. Radiol.* **1992**, *45*, 240.
[51] J.-D. Hecq, A. L. Lewis, D. Vanbeckbergen, A. Athanosopoulos, L. Galanti, J. Jamart, P. Czuczman, T. Chung, *J. Oncol. Pharm. Pract.* **2013**, *19*, 65.
[52] a) J. Kaiser, J. Thiesen, I. Kramer, *J. Oncol. Pharm. Pract.* **2009**, *16*, 53; b) P. L. Pereira, S. Plotkin, R. Yu, A. Sutter, Y. Wu, C. M. Sommer, G. M. Cruise, *Anti-Cancer Drugs* **2016**, *27*, 873.
[53] A. Laurent, J. J. Durussel, J. Dufaux, L. Penhouët, A. L. Bailly, M. Bonneau, J. J. Merland, *CVIR* **1999**, *22*, 62.
[54] A. Laurent, R. Beaujeux, M. Wassef, D. Rüfenacht, E. Boschetti, J. J. Merland, *AJNR* **1996**, *17*, 533.
[55] D. F. Kallmes, J. K. McGraw, A. J. Evans, J. M. Mathis, R. W. Hergenrother, M. E. Jensen, H. J. Cloft, M. Lopes, J. E. Dion, *AJNR* **1997**, *18*, 1243.
[56] T. Das, D. Carugo, X. Zhang, S. Chakraborty, *J. Appl. Phys.* **2012**, *112*, 124701.
[57] a) K. C. Beck, *J. Appl. Physiol.* **1987**, *63*, 883; b) R. J. Domenech, J. I. Hoffman, M. I. Noble, K. B. Saundsers, J. R. Henson, S. Subijanto, *Circ. Res.* **1969**, *25*, 581; c) B. Morgan, A. S. Kennedy, V. Lewington, B. Jones, R. A. Sharma, *Nat. Rev. Clin. Oncol.* **2011**, *8*, 115.
[58] a) C. A. Basciano, C. Kleinstreuer, A. S. Kennedy, *J. Nucl. Med. Radiat. Ther.* **2011**, *2*, 2; b) A. L. Richards, C. Kleinstreuer, A. S. Kennedy, E. Childress, G. D. Buckner, *IEEE Trans. Biomed. Eng.* **2012**, *59*, 198.
[59] a) A. Hoven, J. Prince, M. Samim, A. Arepally, B. Zonneberg, M. E. H. Lam, M. A. J. Bosch, *CVIR* **2014**, *37*, 523; b) S. Rose, S. Kikolski, J. Chomas, *CVIR* **2013**, *36*, 1262.
[60] A. F. Van Den Hoven, M. G. Lam, S. Jernigan, M. A. Van Den Bosch, G. D. Buckner, *J. Exp. Clin. Cancer Res.* **2015**, *34*, 1.
[61] a) K. V. Sharma, M. R. Dreher, Y. Tang, W. Pritchard, O. A. Chiesa, J. Karanian, J. Peregoy, B. Orandi, D. Woods, D. Donahue, J. Esparza, G. Jones, S. L. Willis, A. L. Lewis, B. J. Wood, *JVIR* **2010**, *21*, 865; b) C. G. Johnson, Y. Tang, A. Beck, M. R. Dreher, D. L. Woods, A. H. Negussie, D. Donahue, E. B. Levy, S. L. Willis, A. L. Lewis, B. J. Wood, K. V. Sharma, *JVIR* **2016**, *27*, 117.
[62] X.-J. Lu, Y. Zhang, D.-C. Cui, W.-J. Meng, L.-R. Du, H.-T. Guan, Z.-Z. Zheng, N.-Q. Fu, T.-S. Lv, L. Song, Y.-H. Zou, W.-L. Lu, T.-Y. Fan, *Int. J. Pharm.* **2013**, *452*, 211.
[63] C. G. Johnson, K. V. Sharma, E. B. Levy, D. L. Woods, A. H. Morris, J. D. Bacher, A. L. Lewis, B. J. Wood, M. R. Dreher, *JVIR* **2015**, *27*, 133.
[64] E. B. Levy, C. G. Johnson, G. Jacobs, D. L. Woods, K. V. Sharma, J. D. Bacher, A. L. Lewis, M. R. Dreher, B. J. Wood, *JVIR* **2015**, *26*, 1567.
[65] a) D. H. Choe, M. H. Han, G. H. Kang, K. M. Yeon, M. C. Han, *Invest. Radiol.* **1997**, *32*, 260; b) R. Martin, J. Irurzun, J. Munchart, I. Trofimov, A. Scupchenko, C. Tatum, G. Narayanan, *Korean J. Hepatol.* **2011**, *17*, 51; c) J. Lammer, K. Malagari, T. Vogl, F. Pilleul, A. Denys, A. Watkinson, M. Pitton, G. Sergent, T. Pfammatter, S. Terraz, Y. Benhamou, Y. Avajon, T. Gruenberger, M. Pomoni, H. Langenberger, M. Schuchmann, J. Dumortier, C. Mueller, P. Chevallier, R. Lencioni, *CVIR* **2010**, *33*, 41; d) D. K. Reyes, J. A. Vossen, I. R. Kamel, N. S. Azad, T. A. Wahlin, M. S. Torbenson, M. A. Choti, J.-F. H. Geschwind, *Cancer J.* **2009**, *15*, 526; e) K. Malagari, M. Pomoni, A. Kelekis, A. Pomoni, S. Dourakis, T. Spyridopoulos, H. Moschouris, E. Emmanouil, S. Rizos, D. Kelekis, *CVIR* **2010**, *33*, 541.
[66] a) A. Gholamrezanezhad, S. Mirpour, J.-F. H. Geschwind, P. Rao, R. Loffroy, O. Pellerin, E. A. Liapi, *Eur. Radiol.* **2016**, *26*, 3474; b) O. Akinwande, P. Philips, P. Duras, S. Pluntke, C. Scoggins, R. G. Martin, *CVIR* **2015**, *38*, 361.
[67] R. López-Benítez, G. M. Richter, H.-U. Kauczor, S. Stampfl, J. Kladeck, B. A. Radeleff, M. Neukamm, P. J. Hallscheidt, *CVIR* **2009**, *32*, 615.
[68] G. M. Tozer, S. M. Ameer-Beg, J. Baker, P. R. Barber, S. A. Hill, R. J. Hodgkiss, R. Locke, V. E. Prise, I. Wilson, B. Vojnovic, *Adv. Drug Delivery Rev.* **2005**, *57*, 135.
[69] A. S. Popel, P. C. Johnson, *Annu. Rev. Fluid Mech.* **2005**, *37*, 43.
[70] A. Pries, T. W. Secomb, P. Gaehtgens, *Cardiovasc. Res.* **1996**, *32*, 654.
[71] S. R. Jernigan, J. A. Osborne, C. J. Mirek, G. Buckner, *JVIR* **2015**, *26*, 897.
[72] C. Basciano, C. Kleinstreuer, A. Kennedy, W. Dezarn, E. Childress, *Ann. Biomed. Eng.* **2010**, *38*, 1862.
[73] Z. Xu, S. Jernigan, C. Kleinstreuer, G. D. Buckner, *Ann. Biomed. Eng.* **2016**, *44*, 1036.
[74] M. Caine, X. Zhang, M. Hill, P. Garcia, S. L. Willis, T. Chung, A. L. Lewis, M. R. Dreher, T. de Baere, presented at *World Conf. on Interventional Oncology*, Poster *25*, New York, May **2015**.
[75] a) M. Caine, L. Capretto, D. Carugo, X. Zhang, M. Hill, S. L. Willis, M. R. Dreher, A. L. Lewis, presented at *456th OMICS Int. Biomaterials Conf.*, London, Mar **2016**; b) M. Caine, P. Garcia, Y. Tang, S. L. Willis, M. R. Dreher, A. L. Lewis, presented at *Biomaterials Conf. 2016*, London, March **2016**.
[76] M. Caine, M. S. McCafferty, S. McGhee, P. Garcia, W. M. Mullett, X. Zhang, M. Hill, M. R. Dreher, A. L. Lewis, *J. Vasc. Interv. Radiol.* **2016**, *28*, 260.
[77] D. Carugo, L. Capretto, S. Willis, A. Lewis, D. Grey, M. Hill, X. Zhang, *Biomed. Microdevices* **2012**, *14*, 153.
[78] a) D. Carugo, L. Capretto, B. Roy, M. Carboni, M. Caine, A. L. Lewis, M. Hill, S. Chakraborty, X. Zhang, *J. Controlled Release* **2015**, *214*, 62; b) D. Carugo, *Ph.D. Thesis*, University of Southampton **2012**, p. 297.
[79] a) M. V. Gonzalez, Y. Tang, G. Phillips, A. Lloyd, B. Hall, P. Stratford, A. Lewis, *J. Mater. Sci.: Mater. Med.* **2008**, *19*, 767; b) I. R. Dubbelboer, E. Lilienberg, E. Ahnfelt, E. Sjögren, N. Axén, H. Lennernäs, *Ther. Delivery* **2014**, *5*, 447.

© 2017 WILEY-VCH Verlag GmbH & Co. KGaA, Weinheim

[80] a) M. Biondi, S. Fusco, A. L. Lewis, P. A. Netti, *J. Biomater. Sci., Polym. Ed.* **2012**, *23*, 333; b) M. Biondi, S. Fusco, A. L. Lewis, P. A. Netti, *J. Mater. Sci.: Mater. Med.* **2013**, *24*, 2359.
[81] L. J. Waters, T. S. Swaine, A. L. Lewis, *Int. J. Pharm.* **2015**, *493*, 129.
[82] a) J. Namur, *Ph.D. Thesis*, University of Reims, **2009**; b) J. Namur, M. Wassef, J. P. Pelage, A. Lewis, M. Manfait, A. Laurent, *J. Controlled Release* **2009**, *135*, 198.
[83] J. Namur, M. Wassef, J. M. Millot, A. L. Lewis, M. Manfait, A. Laurent, *JVIR* **2010**, *21*, 259.
[84] A. L. Lewis, M. R. Dreher, *J. Controlled Release* **2012**, *161*, 338.
[85] F. Amyot, V. Boudy, K. Jurski, J. L. Counord, G. Guiffant, J. Dufaux, J. C. Chaumeil, *ITBM-RBM* **2002**, *23*, 285.
[86] T. Borovac, J. P. Pelage, A. Kasselouri, P. Prognon, G. Guiffant, A. Laurent, *J. Controlled Release* **2006**, *115*, 266.
[87] a) K. Fuchs, P. E. Bize, A. Denys, G. Borchard, O. Jordan, *Int. J. Pharm.* **2015**, *482*, 68; b) J. V. Andhariya, D. J. Burgess, *Expert Opin. Drug Delivery* **2016**, *13*, 593; c) T. de Baere, S. Plotkin, R. Yu, A. Sutter, Y. Wu, G. M. Cruise, *JVIR* **2016**, *27*, 1425.
[88] E. Ahnfelt, E. Sjogren, P. Hansson, H. Lennernas, *J. Pharm. Sci.* **2016**, *105*, 3387.
[89] E. Lilienberg, C. E. Barbier, R. Nyman, M. Hedeland, U. Bondesson, N. Axen, H. Lennernas, *Mol. Pharm.* **2014**, *11*, 131.
[90] T. Swaine, Y. Tang, P. Garcia, J. John, L. J. Waters, A. L. Lewis, *Eur. J. Pharm. Sci.* **2016**, *93*, 351.
[91] R. E. J. Forster, S. A. Small, Y. Tang, C. L. Heaysman, A. W. Lloyd, W. Macfarlane, G. J. Phillips, M. D. Antonijevic, A. L. Lewis, *J. Mater. Sci.: Mater. Med.* **2010**, *21*, 2683.
[92] a) K. O. Hicks, F. B. Pruijn, T. W. Secomb, M. P. Hay, R. Hsu, J. M. Brown, W. A. Denny, M. W. Dewhirst, W. R. Wilson, *J. Natl. Cancer Inst.* **2006**, *98*, 1118; b) J. H. Sung, C. Kam, M. L. Shuler, *Lab Chip* **2010**, *10*, 446; c) A. Hagan, W. Macfarlane, A. Lloyd, G. Phillips, R. Holden, Z. Bascal, R. Whomsley, H. Kilpatrick, Y. Tang, A. Lewis, *JVIR* **2016**, *3*, S84.
[93] N. K. Inamdar, J. T. Borenstein, *Curr. Opin. Biotechnol.* **2011**, *22*, 681.
[94] R. A. Sharma, R. Plummer, J. K. Stock, T. A. Greenhalgh, O. Ataman, S. Kelly, R. Clay, R. A. Adams, R. D. Baird, L. Billingham, S. R. Brown, S. Buckland, H. Bulbeck, A. J. Chalmers, G. Clack, A. N. Cranston, L. Damstrup, R. Ferraldeschi, M. D. Forster, J. Golec, R. M. Hagan, E. Hall, A.-R. Hanauske, K. J. Harrington, T. Haswell, M. A. Hawkins, T. Illidge, H. Jones, A. S. Kennedy, F. McDonald, T. Melcher, J. P. B. O'Connor, J. R. Pollard, M. P. Saunders, D. Sebag-Montefiore, M. Smitt, J. Staffurth, I. J. Stratford, S. R. Wedge, *NCRI CTRad Academia-Pharma Joint Working Group, Nat. Rev. Clin. Oncol.* **2016**, *13*, 627.
[95] a) K. Fuchs, A. Kiss, P. Bize, R. Duran, A. Denys, G. Hopfgartner, G. Borchard, O. Jordan, poster presented at *Controlled Release Society*, Seattle, WA, July **2016**; b) K. Fuchs, *Ph.D. Thesis*, University of Geneva **2016**.
[96] J. Namur, S. J. Citron, M. T. Sellers, M. H. Dupuis, M. Wassef, M. Manfait, A. Laurent, *J. Hepatol.* **2011**, *55*, 1332.
[97] D. Domurado, P. Fournié, C. Braud, M. Vert, P. Guérin, F. Simonnet, *J. Bioact. Compat. Polym.* **2003**, *18*, 23.
[98] A. Shmulewitz, R. Langer, *Nat. Biotechnol.* **2006**, *24*, 277.

© 2017 WILEY-VCH Verlag GmbH & Co. KGaA, Weinheim